PLOS COMPUTATIONAL BIOLOGY

RESEARCH ARTICLE

Effect of synchronization of firings of different motor unit types on the force variability in a model of the rat medial gastrocnemius muscle

Rositsa Raikova[1]*, Vessela Krasteva[1], Piotr Krutki[2], Hanna Drzymała-Celichowska[2], Katarzyna Kryściak[2], Jan Celichowski[2]

1 Institute of Biophysics and Biomedical Engineering, Bulgarian Academy of Sciences, Sofia, Bulgaria,
2 Department of Neurobiology, Poznan University of Physical Education, Poznan, Poland

* rosi.raikova@biomed.bas.bg

Citation: Raikova R, Krasteva V, Krutki P, Drzymała-Celichowska H, Kryściak K, Celichowski J (2021) Effect of synchronization of firings of different motor unit types on the force variability in a model of the rat medial gastrocnemius muscle. PLoS Comput Biol 17(4): e1008282. https://doi.org/10.1371/journal.pcbi.1008282

Editor: Hugues Berry, Inria, FRANCE

Received: August 20, 2020

Accepted: April 7, 2021

Published: April 26, 2021

Data Availability Statement: All relevant data are within the manuscript and its Supporting Information files.

Funding: The authors received no specific funding for this work.

Competing interests: The authors have declared that no competing interests exist.

Abstract

The synchronized firings of active motor units (MUs) increase the oscillations of muscle force, observed as physiological tremor. This study aimed to investigate the effects of synchronizing the firings within three types of MUs (slow—S, fast resistant to fatigue–FR, and fast fatigable–FF) on the muscle force production using a mathematical model of the rat medial gastrocnemius muscle. The model was designed based on the actual proportion and physiological properties of MUs and motoneurons innervating the muscle. The isometric muscle and MU forces were simulated by a model predicting non-synchronized firing of a pool of 57 MUs (including 8 S, 23 FR, and 26 FF) to ascertain a maximum excitatory signal when all MUs were recruited into the contraction. The mean firing frequency of each MU depended upon the twitch contraction time, whereas the recruitment order was determined according to increasing forces (the size principle). The synchronization of firings of individual MUs was simulated using four different modes and inducing the synchronization of firings within three time windows (± 2, ± 4, and ± 6 ms) for four different combinations of MUs. The synchronization was estimated using two parameters, the correlation coefficient and the cross-interval synchronization index. The four scenarios of synchronization increased the values of the root-mean-square, range, and maximum force in correlation with the increase of the time window. Greater synchronization index values resulted in higher root-mean-square, range, and maximum of force outcomes for all MU types as well as for the whole muscle output; however, the mean spectral frequency of the forces decreased, whereas the mean force remained nearly unchanged. The range of variability and the root-mean-square of forces were higher for fast MUs than for slow MUs; meanwhile, the relative values of these parameters were highest for slow MUs, indicating their important contribution to muscle tremor, especially during weak contractions.

Author summary

The synchronization of firings of motor units (MUs), the smallest functional elements of skeletal muscle increases fluctuations in muscle force, known as physiological tremor, which can disturb high-precision movements. In this study, we adopted a recently proposed muscle model consisting of MUs of three different types (fast fatigable, fast resistant to fatigue, and slow) to study four different scenarios of MU synchronization during a steady level of excitatory input to motoneurons. The discharge patterns were synchronized between pairs of MUs by shifting in time individual pulses, which occurred within a short time interval, and a degree of synchronization was then estimated. The increased synchronization index resulted in increased force variability for all MU types as well as for the whole muscle output; however, the mean force levels remained nearly unchanged, whereas the frequencies of the force oscillations were decreased. The absolute range of force variability was higher for fast than for slow MUs, indicating their dominant influence on muscle tremor at strong contractions, but the highest relative increase in force variability was observed for synchronized slow MUs, indicating their significant contribution to tremor during weak contractions, in which only slow MUs are active.

Introduction

Most studies of motor unit (MU) firings have revealed the existence of a certain level of synchronization between the firings of motoneurons innervating the same muscle [1–4]. Two concepts for long- and short-term synchronization can be found in the literature. Long-term synchronization with greater latencies beyond ± 20 ms was reported by Datta and Stephens, De Luca et al., Kirkwood et al., Schmied et al., and Semmler et al. [1,4–7]. The possible mechanism of this kind of synchronization could be explained as interactions occurring between the stretch reflex loop and the recurrent inhibition. Long-term synchronization has been reported to be relatively rare in comparison to short-term synchronization [4], which was reported to be a peak in the cross-interval histogram centered about a zero-time delay (0.5 ± 2.9 ms). Short-term synchronization is attributed to last-order projections that provide common, nearly simultaneous, excitatory synaptic input across motoneurons [3,8,9,10], generating a narrow peak around the origin of the cross-correlogram of MU discharges [1,8,11,12]. Therefore, the narrow synchronous peak principally reflects shared, monosynaptic projections to motor neurons from corticomotoneuronal cells via the lateral corticospinal tract [13].

In humans, the MU synchronization was shown to be stronger during voluntary muscle activation than during reflex activation [14]. At the same time, synchronization tends to be higher in more distally located muscles, while the greatest synchrony has been most often found in the intrinsic muscles of the foot rather than in the hand muscles [3,15]. However, the level of synchronization between MUs could be influenced by numerous factors, such as the examined task, the muscles involved in the task, and the type of habitual physical activity performed by the individual [6–7,16–19]. For example, the level of synchronization was reduced between MUs in the hand muscles of individuals who required greater independent control of the fingers. This included musicians [18] and the dominant hands of control subjects [7]. On the other hand, MU synchronization was found to be greater in the hand muscles of individuals who consistently performed strength training [18,20] or during tasks that demanded attention [21]. The enhancement of MU synchronization was observed after daily exercise involving brief periods of maximal muscular contraction [20] and contributed to training-induced increments in muscle strength [22]. Greater synchronization has also been noted in

fatigued muscles [23]. Reports regarding the relationship between physiological tremor and synchronization are inconsistent: most of them have linked tremor with an increased level of synchronization [23–26], while others have suggested no significant associations between the tremor amplitude and the level of MU synchronization exist [18].

It has been assumed that muscle can produce smooth contractions due to asynchronous discharges of motor neurons [24]. Yao et al. [22] revealed that MU synchronization increased the variability in the simulated force but not the average force. Synchronization was also shown to increase the estimated twitch force and decrease the contraction time of the MUs [27], though it was likely a result of inaccurate measure of MU twitch properties in that model.

In the majority of skeletal muscles, three types of MUs have been distinguished and their contractile properties, including the force–frequency of stimulation relationship [28] and sensibility to changes in stimulation pattern [29,30], were found to vary considerably. In several studies, the effects of the synchronization of MU firings were modeled [22,31,32]; however, these models did not analyze the specific effects attributable to different types of MUs. In our previous paper [33], a model of the rat medial gastrocnemius muscle consisting of 30 MUs [10 MUs each of the fast fatigable (FF), fast resistant to fatigue (FR), and slow (S) types] was proposed and the effects of synchronous and asynchronous stimulation of MUs were investigated. It was concluded that the activation of MUs at variable interpulse intervals, delivered to each MU asynchronously, resulted in smaller force oscillations. However, the study did not assess the effects of synchronization between pairs of individual MUs nor the effects of the synchronization of three types of MUs.

A recent model of the rat medial gastrocnemius muscle [34] provided methodology by which to identify the role of each of three MU types (FF, FR, and S) in the production of muscle force. In the present study, the same model was adopted as a tool for simulation of four modes and three time levels of synchronization. The aim of this research was to reveal the effects of synchronization of firing within the three types of MUs on the force variability and the force mean spectral frequency and to compare these effects between different types of MUs and the whole muscle. The implication of the results for explanation of tremor at various levels of the muscle force was discussed.

Materials and methods

Muscle model

This study applied a model of the rat muscle gastrocnemius based on excitability and firing frequencies of motoneurons, contractile properties, and the number and proportion of MUs in the muscle [34]. Briefly, the model consisted of 57 MUs, including eight S, 23 FR, and 26 FF MUs, respectively. Their basic contractile properties are presented in Table 1. As input data, this set of MUs, recorded in physiological experiments, was selected and their twitches were precise modeled by a six-parameter analytical function dependent on time [35]. These twitches are given in Fig 1 in Raikova et al. (2018) [34]. The muscle force was calculated as the sum of forces of all active MUs and the process of force regulation was set according to the common-drive hypothesis [36]. The muscle unfused tetanus was calculated following the application of a train of irregular stimuli and was simulated using an analytical approach described in previous researches [34,37]. The tetanic force of each MU was calculated as a sum of unequal twitches analytically described by the 6-parameters analytical function. These parameters were changeable and were computed using regression equations derived by decomposition of tetanic curves recorded in physiological experiments for 30 MUs [37]. Meanwhile, the scheme of MU firing was adopted from Fuglevand et al. [31].

Table 1. Main input data for the muscle model: values of the basic contractile properties of the 57 MUs (slow, S1–S8; fast resistant to fatigue FR1–FR23; fast fatigable FF1–FF26) selected for the muscle modeling and their firing properties. T_c–the contraction time; T_{hr}–the half-relaxation time; T_{tw}–the duration of the twitch; F_{max}–the maximum force of the twitch; F_{mftf}–the maximum force of the fused tetanus; ***meanfr***–the mean frequency of rhythmic firing; ***minfr***–the minimum rhythmic firing frequency; ***maxfr***–the maximum rhythmic firing frequency. Data are taken from Table 1 in Raikova et al. [33].

MU number	MU type	T_c (ms)	T_{hr} (ms)	T_{tw} (ms)	F_{max} (mN)	F_{mftf} (mN)	*meanfr* (Hz)	*minfr* (Hz)	*maxfr* (Hz)
1	S1	28	65.5	160	3.8	32.35	26.9	13	38.2
2	S2	24	54	120	5.1	64.96	43.7	17.5	58.9
3	S3	22	54	110	5.3	75.03	47.8	18.6	64
4	S4	24	53	120	5.5	67.64	39.5	16.4	53.7
5	S5	24	55	120	6.5	69.35	35.3	15.3	48.5
6	S6	24	61	150	6.5	48.6	31.1	14.1	43.3
7	S7	36	82	170	7.8	66.67	22.8	11.9	33
8	S8	21.5	46	121	11	38.4	52	19.7	69.2
9	FR1	14	28	69.7	2.1	17.86	58.7	29.7	104
10	FR2	12.3	22.3	50.5	3	26.19	72.2	36.1	129.6
11	FR3	13	24	55.1	7.75	44.05	70.3	35.2	126
12	FR4	15.8	33	85	8.1	45.33	43.4	22.4	74.7
13	FR5	15.3	32.7	86	9	44.26	47.2	24.3	82
14	FR6	16	34	81.8	10.2	50.55	41.5	21.5	71.1
15	FR7	11.8	19.5	60	12.2	76.56	74.1	37	133.3
16	FR8	19.5	41.3	107.8	12.9	50.18	33.8	17.9	56.4
17	FR9	13	22.3	47.5	14.1	73.99	68.3	34.3	122.3
18	FR10	20.8	42.5	99	14.2	46.52	31.9	17	52.7
19	FR11	13.5	25	57.5	14.5	99.76	66.4	33.4	118.6
20	FR12	14.8	26.5	59	14.8	80.4	49.2	25.2	85.7
21	FR13	13.8	22.8	46.5	15.8	70.94	60.7	30.6	107.7
22	FR14	17	36	94	17	105.3	37.7	19.7	63.7
23	FR15	15.4	33.5	82.2	18	75.46	45.3	23.4	78.4
24	FR16	18.5	43	160	21	79.87	35.7	18.8	60.1
25	FR17	14	26.9	80	23	146	56.8	28.8	100.3
26	FR18	13.5	28.4	160	23.7	114.7	64.5	32.5	115
27	FR19	14.3	33	160	26.6	103.6	53	27	93
28	FR20	16.3	36	85	30.67	201.1	39.6	20.6	67.4
29	FR21	14	29.5	67	56	159	54.9	27.9	96.7
30	FR22	13.5	27.5	65	70.5	184.1	62.6	31.6	111.3
31	FR23	14.7	30.6	80	78.3	275	51.1	26.1	89.4
32	FF1	12.5	21	42.5	5.9	43.53	67.4	33.8	120.4
33	FF2	12.9	22	46.5	9.7	34.69	64	32.2	114
34	FF3	12.2	21.8	48.5	11.4	42.31	69	34.6	123.6
35	FF4	13	21.5	44	13.5	92.55	62.3	31.4	110.7
36	FF5	11.8	23.1	56	14.8	81.5	72.4	36.2	130.1
37	FF6	13.5	25.8	61.3	18.4	98.05	53.8	27.4	94.6
38	FF7	12	22.8	54	18.6	63.37	70.7	35.4	126.9
39	FF8	15	30.5	70.8	22.2	75.58	38.6	20.2	65.6
40	FF9	13.4	25.4	60	22.7	86.1	55.5	28.2	97.8
41	FF10	13.3	25.8	62	29	110.6	57.2	29	101.1
42	FF11	11.5	23	57.2	32.2	97.25	74.1	37	133.3
43	FF12	15.7	31.2	71	33.5	112	35.3	18.6	59.2
44	FF13	17.5	36.3	85.5	33.8	89.8	33.6	17.8	56

(*Continued*)

Table 1. (Continued)

MU number	MU type	T_c (ms)	T_{hr} (ms)	T_{tw} (ms)	F_{max} (mN)	F_{mftf} (mN)	*meanfr* (Hz)	*minfr* (Hz)	*maxfr* (Hz)
45	FF14	13	21.5	43.8	38.2	149.6	60.6	30.6	107.5
46	FF15	12.6	21	43.3	41.4	191.1	65.7	33	117.2
47	FF16	13.9	25.2	57	54.1	186.3	48.8	25	85
48	FF17	14	25	55.5	57.7	178.9	47.1	24.2	81.7
49	FF18	15	24.6	60	63.4	155	37	19.4	62.4
50	FF19	18.5	38	80	84.3	322.9	31.9	17	52.7
51	FF20	13.7	29.2	70	97.6	231	52.2	26.6	91.4
52	FF21	14.5	31	70	121.4	295.7	42	21.8	72.1
53	FF22	13.8	26.5	70	129.5	284.7	50.5	25.8	88.2
54	FF23	14.5	29.6	61	130	220	40.3	21	68.8
55	FF24	14.2	28.5	60	141	456.1	43.7	22.6	75.3
56	FF25	14	31	70	170.3	510.9	45.4	23.4	78.5
57	FF26	13	31	69	175	382.4	58.9	29.8	104.3

https://doi.org/10.1371/journal.pcbi.1008282.t001

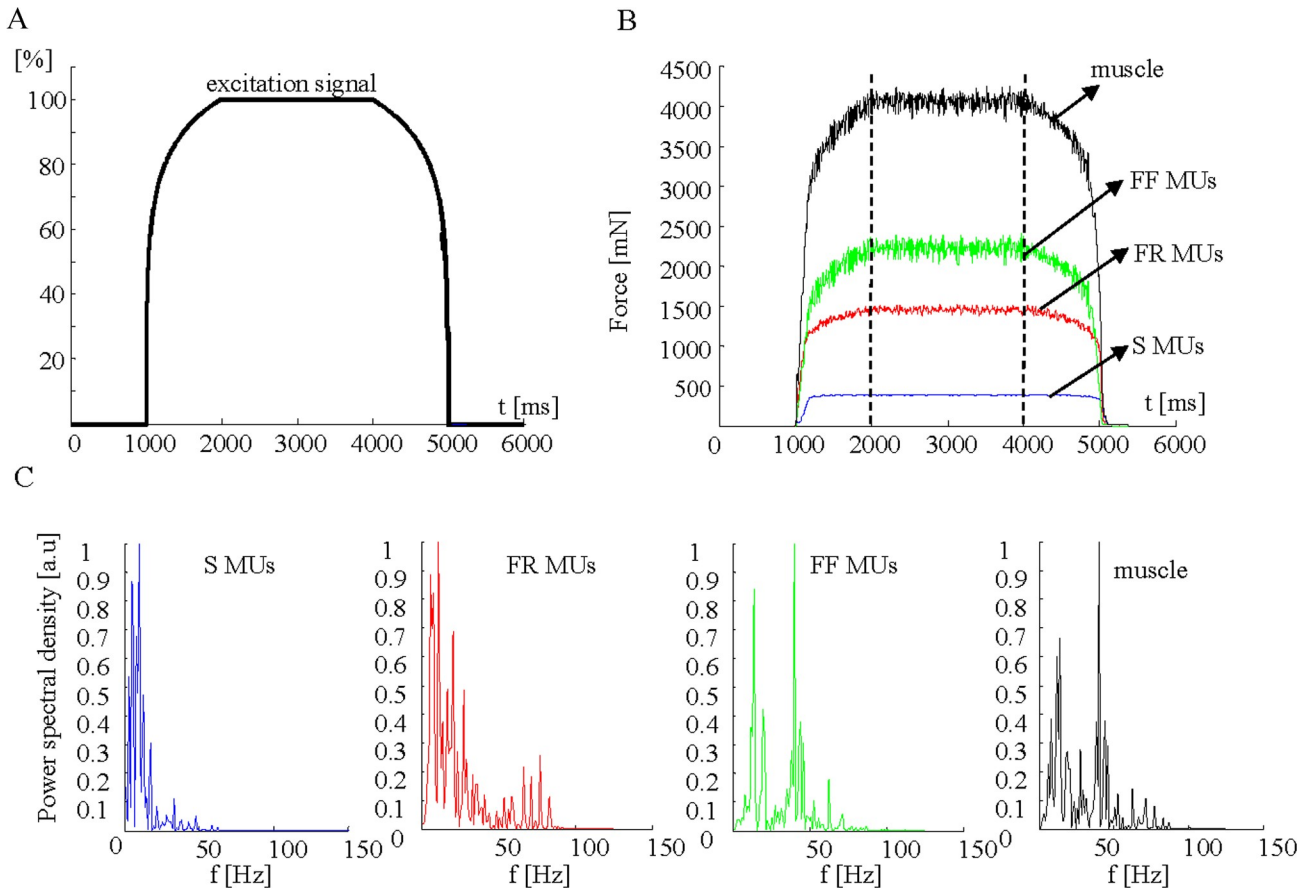

Fig 1. Parameters of the basic model, calculated using a 100% excitation signal. A. The law for the excitation. B. The calculated forces of populations of different MU types (S, FR, and FF) and the muscle. C. Normalized power spectral density of the force during a time period of 2000 to 4000 ms, presented separately for individual MUs (S, FR, and FF) and the whole muscle.

https://doi.org/10.1371/journal.pcbi.1008282.g001

In the present study, the excitation signal was simulated (Fig 1A) as consisting of two smooth logarithmic parts during the rising and falling slopes of the muscle force (each lasting 1000 ms) and a straight line during the steady state of the muscle (lasting 2000 ms). The shape of the signal waveform was designed to better approximate more realistically a course of excitation input to motoneurons, avoiding sudden changes occurring in any trapezoidal signal used previously. This study considered only one excitation level, corresponding to 100% of the activation signal, ensuring that all MUs were activated during the steady state of the muscle to enable a thorough analysis of their synchronization. The program for simulation of the force MUs and the muscle force accepted the same MU firing frequencies as previously described [34] (Table 1). The interpulse intervals (IPIs) were calculated by generator of uniformly distributed pseudorandom numbers within the interval of ±4 ms around the IPI corresponding to the mean frequency of each MU. The simulated train of firings at random IPIs are presented in a supplementary table (S1 Data). IPIs histograms are also presented in a supplementary figure (S1 Fig) demonstrating IPIs uniform distribution. Finally, the model generated the output forces for different MUs (S, FR, and FF) and the whole muscle, as illustrated in Fig 1B (sampling frequency fs = 1 kHz) and raw data presented in the supplement (S2 Data). This was further denoted as the basic (non-synchronized; *NS*) model, to which no attempts of manual changes of MU firing for synchronization were applied. The force signals were analyzed during the steady-state periods (2000–4000 ms). Their power frequency spectra were calculated by using fast Fourier transform (FFT) over nf = 2048 points, thus achieving a spectral resolution $\Delta f = fs/nf$ = 0.49 Hz (Fig 1C).

Simulation of MU synchronization

The *NS* firings of all 57 MUs during the muscle steady state are shown in Fig 2 and presented in a supplementary table (S1 Data). These patterns were further modified to simulate different types and levels of synchronization. The synchronization was applied to a specific pair of MUs (named MU1 and MU2) so that the pulses of MU2, which fall within a predefined time window, Δt, around the pulses of MU1, were changed to coincide with those of MU1. Three time windows with $\Delta t = \pm 2, \pm 4$ or ± 6 ms were used to simulate three levels of MU synchronization, mimicking weak, modest, and strong synchronization, respectively. The synchronization scheme is illustrated in Fig 3, showing that the larger the time window was, the greater number of MU pulses were shifted to and synchronized with the reference MU.

Four methods of synchronization (Methods 1–4) were applied. In all methods, the synchronized MU pairs were chosen only encompassing the same physiological type (S and S, FR and FR, FF and FF), i.e., synchronization was not induced between MUs of different types.

- *Method 1*: Two neighboring MUs within the same physiological type according to the recruitment order based on their increasing force of the twitch (Table 1) were synchronized, i.e., for S MUs, 1–2, 2′–3, . . ., 7′–8; for FR MUs, 9–10, 10′–11, . . ., 30′–31; and, for FF MUs, 32–33, 33′–34, . . ., 56′–57. Note that, for each next synchronization, the already synchronized pattern of the previous MU is used and marked by "′".
- *Method 2*: Two neighboring MUs within the same physiological type but when ordered according to their increasing mean firing rate (Table 1), were synchronized i.e., for S MUs, 7–1, 1′–6, 6′-5, 5′–4, 4′–2, 2′–3, and 3′–8; for FR MUs, 18–16, 16′–24, 24′–22, 22′–28, 28′–14, 14′–12, 12′–23, 23′–13, 13′–20, 20′–31, 31′–27, 27′–29, 29′–25, 25′–9, 9′–21, 21′–30, 30′–26, 26′–19, 19′–17, 17′–11, 11′–10, and 10′–15; and, for FF MUs, 50–44, 44′–43, 43′–49, 49′–39, 39′–54, 54′–52, 52′–55, 55′–56, 56′–48, 48′–47, 47′–53, 53′–51, 51′–37, 37′–40, 40′–41, 41′–57, 57′–45, 45′–35, 35′–33, 33′–46, 46′–32, 32′–34, 34′–38, 38′–36, and 36′–42.

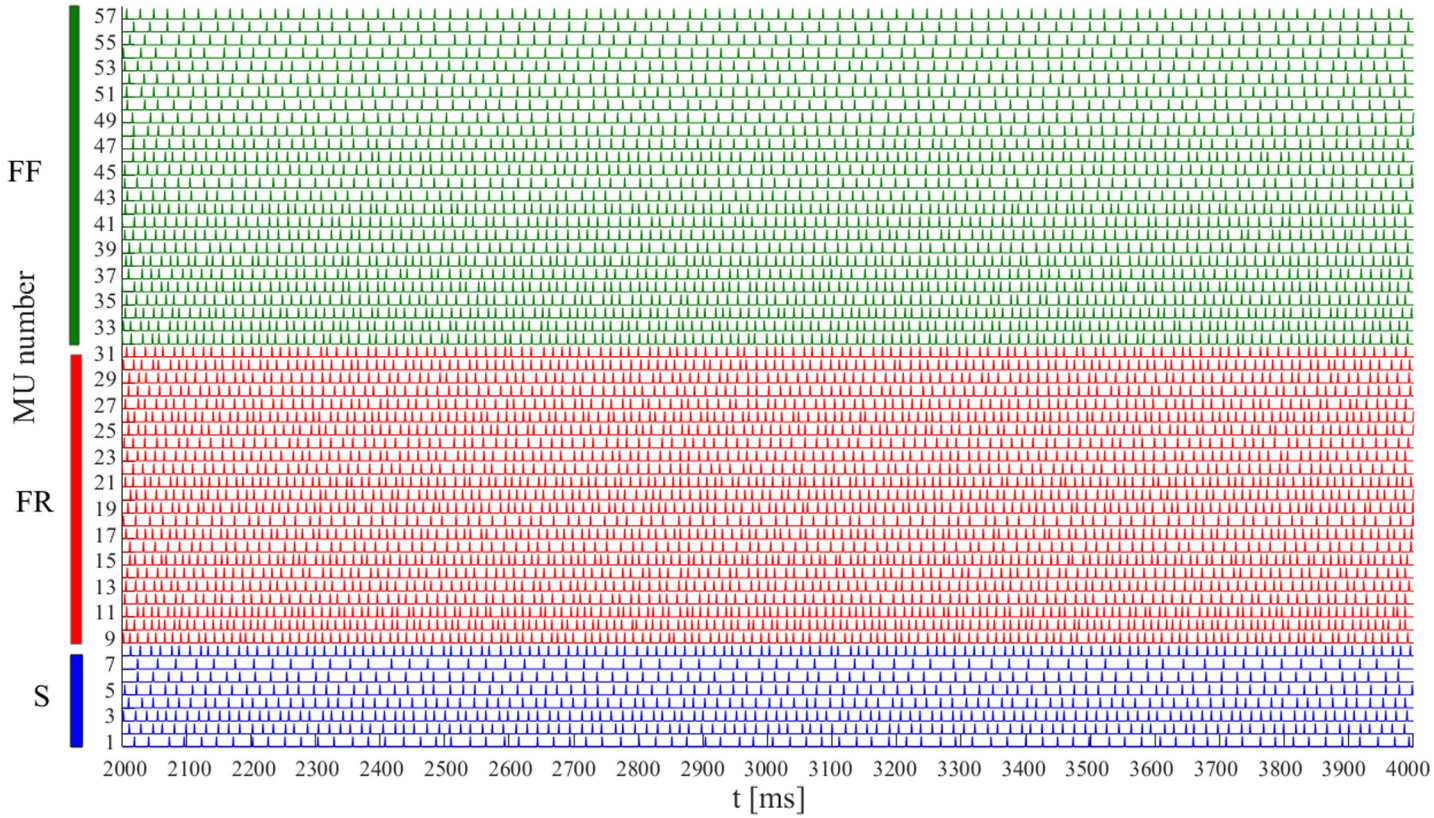

Fig 2. Firing patterns of 57 MU of the basic *NS* model during the time period of 2000 to 4000 ms. MUs are numbered in an ascending order based on their maximum twitch forces within each type: S (1–8), FR (9–31), and FF (32–57).

https://doi.org/10.1371/journal.pcbi.1008282.g002

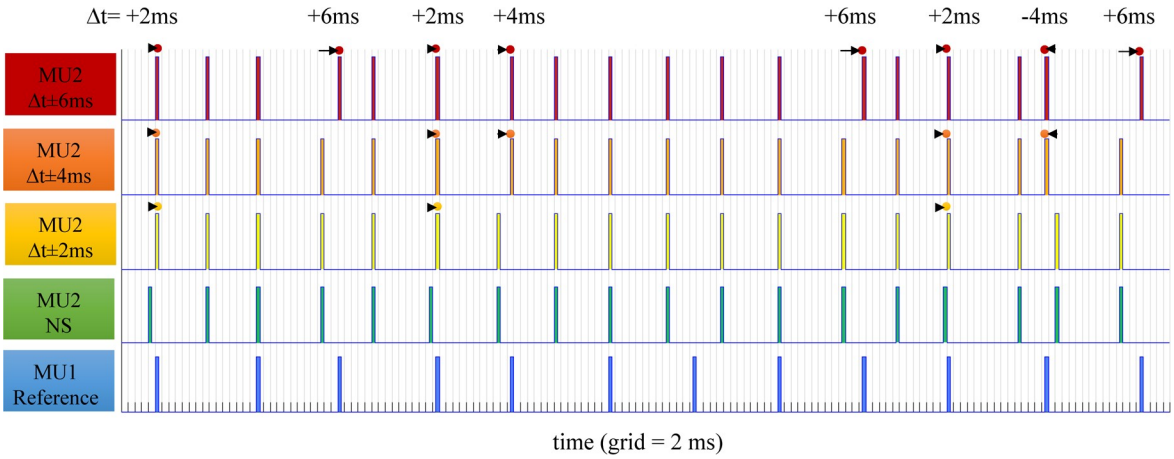

Fig 3. Illustration of the synchronization principle of basic MU firing patterns of two MUs, considering MU1 as a reference one (blue, bottom) and applying the synchronization of pulses to MU2 (green, *NS*). Three time windows were used: $\Delta t = \pm 2$ ms (yellow), ± 4 ms (orange), and ± 6 ms (red). The dots highlight individual pulses of MU2, which were shifted in time (left or right, as indicated by arrows) to coincide with reference impulses of MU1 when the time interval between the pair of impulses of MU2 and MU1 was less or equal than $|\Delta t|$. The level of synchronization was proportional to Δt, illustrated in this example by increasing numbers n of shifted impulses—namely, $n = 3$ for $\Delta t = \pm 2$ ms, $n = 5$ for $\Delta t = \pm 4$ ms, and $n = 8$ for $\Delta t = \pm 6$ ms.

https://doi.org/10.1371/journal.pcbi.1008282.g003

- *Method 3*: The MUs within the same physiological type but in unique groups of four MUs were synchronized to the first recruited MU and ordered according to their increasing force of the twitch (Table 1), i.e., for S MUs, 1–2, 1–3, 1–4, 5–6, 5–7, and 5–8; for FR MUs: 9–10, 9–11, 9–12, 13–14, 13–15, 13–16, 17–18, 17–19, 17–20, 21–22, 21–23, 21–24, 25–26, 25–27, 25–28, 29–30*, and 29–31*; and, for FF MUs, 32–33, 32–34, 32–35, 36–37, 36–38, 36–39, 40–41, 40–42, 40–43, 44–45, 44–46, 44–47, 48–49, 48–50, 48–51, 52–53, 52–54, 52–55, and 56–57*. The symbol (*) denotes the groups, where the number of synchronized MUs was less than four due to the fact that the number of MUs in the respective physiological type was not a multiple of four.
- *Method 4*: The MUs within the same physiological type were synchronized, taking as a reference the first recruited MU of the specific type (Table 1), i.e., for S MUs, 1–2, 1–3, . . ., 1–8; for FR MUs, 9–10, 9–11,. . ., 9–31; and, for FF MUs, 32–33, 32–34, . . ., 32–57.

Estimation of MU synchronization

Temporal correlation of MU pulses. The MU pulses were represented as an MU binary (MUB) sample series with a constant sampling period of 1 ms and binary amplitude of 0 or 1, where "0" indicated a non-active state and "1" indicated the presence of a pulse-active state. The duration of the pulse-active state was set to 1 ms, overlaying one sampling period. MUB series were represented with a total of 2000 samples during the steady state of the muscle from 2000 ms to 4000 ms, as depicted in Figs 1 and 2 for the MUs in the basic, *NS* model.

The temporal correlation between the binary sample series of two MUs (MUB1 and MUB2) was computed with the normalized Pearson's correlation coefficient ranged in the interval 0% to 100%, according to the following formula:

$$corMU = \frac{\sum_{i=2000ms}^{4000ms} MUB1_i \cdot MUB2_i}{\sqrt{\sum_{i=2000ms}^{4000ms} MUB1_i^2 \cdot \sum_{i=2000ms}^{4000ms} MUB2_i^2}} .100[\%], \quad (1)$$

where i denotes the sample index of the MUB series, considering a sampling period of 1 ms.

The correlation coefficient (*corMU*) is a standard measure of similarity between sample series data in the time domain. Transferring this knowledge to the MUB data, *corMU* is representative of the temporal synchronization of two MU firings such that 100% corresponds to a complete coincidence between all firing pulses in MU1 and MU2 and 0% corresponds to no coincidence between any firing pulse in MU1 and MU2. The normalized value of *corMU* does not depend upon the length of the estimated MUB time series, the number of firing pulses, or the mean firing rate. This is an important benefit of the normalization, which would prevent bias in *corMU* estimation, considering that MUs in different physiological types have different mean firing rates.

Cross-interval synchronization index. The synchronization between the firing patterns of two MUs (MU1 and MU2) was estimated by an analysis of their cross-intervals using $CI_x(MU1,MU2) = \{t1_x - t2_{xy}\}$ computed as a pair-wise difference between the times of occurrence of all reference MU1 pulses $t1_x = \{t1_1, t1_2, \ldots t1_{nMU1}\}$ and their corresponding closest neighbors among MU2 pulses $t2_{xy} \in t2_y = \{t2_1, t2_2, \ldots t2_{nMU2}\}$. The latter were found by the minimization criterion $t2_{xy} = \arg\min_{y=1,2,..nMU2}\{|t1_x - t2_y|\}$ and respected the condition to overlay only firings during the steady state of the muscle, i.e., $t1_x, t2_y \in [2000ms; 4000ms]$. By

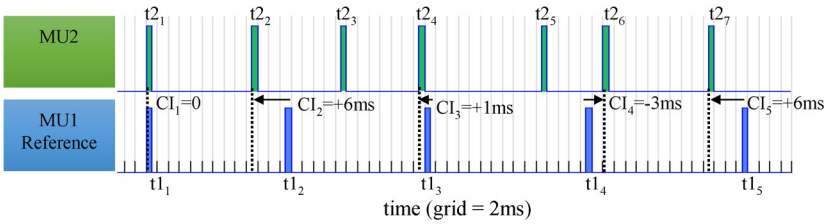

Fig 4. Illustration of the cross-interval measurements of pulses of real MU firing patterns {CI_1, CI_2, CI_3, CI_4, CI_5}, considering MU1 as a reference (blue, bottom) and applying pairwise differences between the times of occurrences of all MU1 pulses {$t1_1$, $t1_2$, $t1_3$, $t1_4$, $t1_5$} and their corresponding closest neighboring pulse times of MU2 {$t2_1$, $t2_2$, $t2_4$, $t2_6$, $t2_7$}.

https://doi.org/10.1371/journal.pcbi.1008282.g004

definition, the $CI_x(MU1,MU2)$ vector length was equal to the number of pulses in the reference MU (nMU1). *CI* values could be negative, zero, or positive when an MU1 pulse was respectively preceding, coinciding with or following its neighbor MU2 pulse, as illustrated in Fig 4.

The distribution of cross-interval values of two MUs, *CI(MU1,MU2)*, was estimated by means of a cross-interval histogram with a bin-width resolution of 1 ms and bin centers in the range of ± 15 ms. The bin values represented the relative probability (p_{bi}) of having a *CI* observation within a specific bin interval (*bi*):

$$p_{bi} = \frac{c_{bi}\{CI(MU1, MU2)\}}{nMU1}, \tag{2}$$

accepting the sum of all bin values equal to 1:

$$\sum_{bi=-15ms}^{+15ms} p_{bi} = 1, \tag{3}$$

where c_{bi} is the count of *CI (MU1,MU2)* values in bin *bi* and the denominator is the number of elements in the input data, equal to the number of reference MU pulses (*nMU1*).

Derived from the cross-interval histogram, the synchronization between the firing patterns of MU1 and MU2 was estimated by the relative probability p_{b0} in the central bin ($b0 = \pm 0.5$ ms), equivalent to the relative frequency of coincidence between MU1 and MU2 pulses related to the reference number of pulses:

$$p_{b0} = \frac{c_{b0}\{-0.5ms \le CI(MU1, MU2) < +0.5ms\}}{nMU1}. \tag{4}$$

Given a total number of $N = 57$ MUs, there could be derived a total of N-1 cross-interval vectors *CI(MUi, MUj)* for any given pair of MUs, where $i, j = 1, 2,.., N$, and $i \neq j$. Further, a cross-interval synchronization index (*CISI*) was defined for each reference MUi pattern to accumulate the relative probability of pulse coincidences in all MUi pairs (N–1) observed in the central bin:

$$CISI(MUi) = \frac{1}{N-1}\sum_{\substack{j=1 \\ j\neq i}}^{N} \frac{c_0\{CI(MUi, MUj)\}}{nMUi}.100[\%], \tag{5}$$

CISI has a normalized value from 0 to 100% with 0% corresponding to no coincidence and 100% corresponding to a complete coincidence between the patterns of the reference MUi and all other paired MUs. The adopted *CISI* normalization to both number of MU pairs (N) and number of reference firings (*nMUi*) was implemented to reject the influence of the size and type of the studied MU population.

Force parameters. Standard force parameters of the different MU groups (S, FR, and FF) and the cumulative force of the whole muscle (Fig 1B) were calculated as follows:

- Force mean value: $meanF = \sum_{i=1}^{n} \frac{F_i}{n}$,
- Force max value: $max\ F = max(F_i)$,
- Force min–max range: $rangeF = max(F_i) – min(F_i)$,
- Force root-mean-square (*RMS*) level: $rmsF = \sqrt{\sum_{i=1}^{n} \frac{(F_i - meanF)^2}{n}}$,

where F_i denoted the force signal samples, taken with a sampling period of 1 ms during the steady state of the muscle from 2000 ms to 4000 ms, including a total number of $n = 2000$ samples.

Furthermore, a variance based parameter, namely percentage of Variance Accounted For (*VAF*), was computed to account the effect of MU synchronization on the variance of differences between synchronized forces (*FS*) and the non-synchronized forces (*FNS*) of the basic, *NS* model:

$$VAF = (1 - \frac{\mathrm{var}(FS_i - FNS_i)}{\mathrm{var}(FNS_i)}).100\%, \quad (6)$$

where *i* denotes the force signal samples from 2000 ms to 4000 ms, var(FS_i-FNS_i) denotes the total sum of squared differences between forces and var(FNS_i) denotes the total sum of squares taken with respect to the mean value. *VAF* was used in literature to estimate the synchronization between forces of different muscles [38,39,40]. *VAF* of two equal forces is 100%. *VAF* is expected to decrease if the variance of the differences between two forces grows due to synchronization.

Additionally, the force power spectral density (*PSD*) of different MU groups (S, FR, and FF) and the cumulative muscle force (Fig 1C) was used for the calculation of the mean spectral frequency as follows:

$$meanfreq = \frac{\sum_{i=1}^{nf} f_i.PSD_i}{\sum_{i-1}^{nf} PSD_i}[Hz], \quad (7)$$

where *nf* is number of frequency bins in the spectrum ($nf = 2048$ as defined earlier), *fi* is the frequency of the spectrum at bin *i* of *nf*, and *PSDi* is the amplitude of the *PSD* at bin *i* of *nf*.

Results

Weak synchronization of MU firings in the basic muscle model

The level of synchronization between MU firing patterns of the simulated basic rat muscle gastrocnemius model with 100% excitation containment and 57 MUs, over a two-second time period during the muscle steady state, was estimated by the two different synchronization indices in Table 2 (top row) and discussed as follows.

First, $corMU = 6.1\% \pm 2.8\%$ (mean value ± standard deviation) shows a ***weak temporal*** correlation between the firing pulses of all MUs within the muscle, which was found to be lowest for MUs of type S (4.5% ± 2%) and highest for those of type FR (7.4% ± 2.9%). A

Table 2. Two indices of synchronization (*corMU* and *CISI*), measured for the NS model and four methods of synchronization (Methods 1–4) within three time windows (± 2, ± 4, and ± 6 ms). All values are reported as mean value ± standard deviation for different physiological types of MUs (S, FR, and FF) and for all MUs within the muscle.

		corMU [%]				*CISI* [%]			
		S MUs	**FR MUs**	**FF MUs**	**all MUs**	**S MUs**	**FR MUs**	**FF MUs**	**all MUs**
NS		**4.5±2.0**	**7.4±2.9**	**5.7±2.8**	**6.1±2.8**	**5.8±0.5**	**6.2±0.4**	**6.2±0.3**	**6.2±0.4**
Method 1	**±2ms**	10.4±7.8	11.5±8.6	8.2±7.6	7.3±5.8	6.4±0.8	7.8±0.6	7.3±0.7	7.4±0.8
	±4ms	21.9±15.2	21.3±16.5	13.4±14.7	10.2±11.4	8.1±0.9	11.7±0.9	9.6±1.6	10.3±1.8
	±6ms	37.2±19.5	38.4±21.1	22.3±22.4	15.0±18.4	8.8±1.0	18.7±1.8	13.9±3.4	15.1±4.3
Method 2	**±2ms**	10.4±9.7	11.4±10.6	8.4±9.0	7.6±6.6	6.7±0.5	8.0±1.0	7.6±0.8	7.6±0.9
	±4ms	20.6±15.7	22.5±19.0	13.9±15.9	10.5±12.5	7.6±0.5	12.3±1.8	10.0±1.8	10.6±2.3
	±6ms	38.1±19.7	39.7±21.5	20.2±21.9	15.2±18.4	10.3±0.8	19.4±3.1	13.3±2.9	15.4±4.5
Method 3	**±2ms**	9.5±7.7	10.0±7.9	7.5±7.5	6.9±5.4	6.4±0.6	7.2±0.4	6.9±0.7	6.9±0.6
	±4ms	15.7±14.8	13.5±16.2	9.9±13.9	7.9±9.9	7.2±0.8	8.4±0.5	7.9±1.2	8.0±1.0
	±6ms	23.8±23.5	16.8±24.3	12.2±20.0	9.1±14.5	8.2±1.0	9.7±0.7	9.0±1.4	9.2±1.2
Method 4	**±2ms**	11.5±6.9	19.5±7.6	16.6±9.3	10.1±8.2	6.3±0.7	10.8±1.6	10.9±1.9	10.2±2.3
	±4ms	24.9±10.6	46.6±9.6	39.3±13.5	19.1±19.5	7.8±1.1	21.4±2.1	21.0±2.4	19.3±5.2
	±6ms	42.6±10.9	74.6±6.9	62.8±13.1	28.3±31.2	9.0±1.4	32.1±1.5	31.6±1.4	28.6±8.1

https://doi.org/10.1371/journal.pcbi.1008282.t002

comprehensive proof for the absence of noteworthy clusters with significant correlation between MUs of a specific type is illustrated in the *corMU* colormap in Fig 5A. Here, a random distribution of *corMU* values can be noted, overlaying the dark-blue colored area of very low pairwise correlations between 57 × 57 MUs, distributed on the *x*- and *y*-axes. The entries in the main diagonal should be ignored because each represents a MU compared with itself (*corMU* = 100%).

Second, *CISI* = 6.2% ± 0.4% (mean value ± standard deviation) suggests ***weak*** cross-interval synchronization between the firing pulses of all MUs within the muscle, without essential differences between MUs of different physiological types [the *CISI* mean value varied from 5.8% (S MUs) to 6.2% (FR and FF MUs)]. Evidence for missing synchronization between MU firings can be observed in the cross-interval histograms in Fig 6A, having a flat (uniform) distribution in the range of bin intervals [−6 ms; +6 ms] for all 57 MUs. Therefore, cross-intervals between firing patterns were equally probable within this bin range and no evidence for synchronous peaks could be identified in the case of any MU.

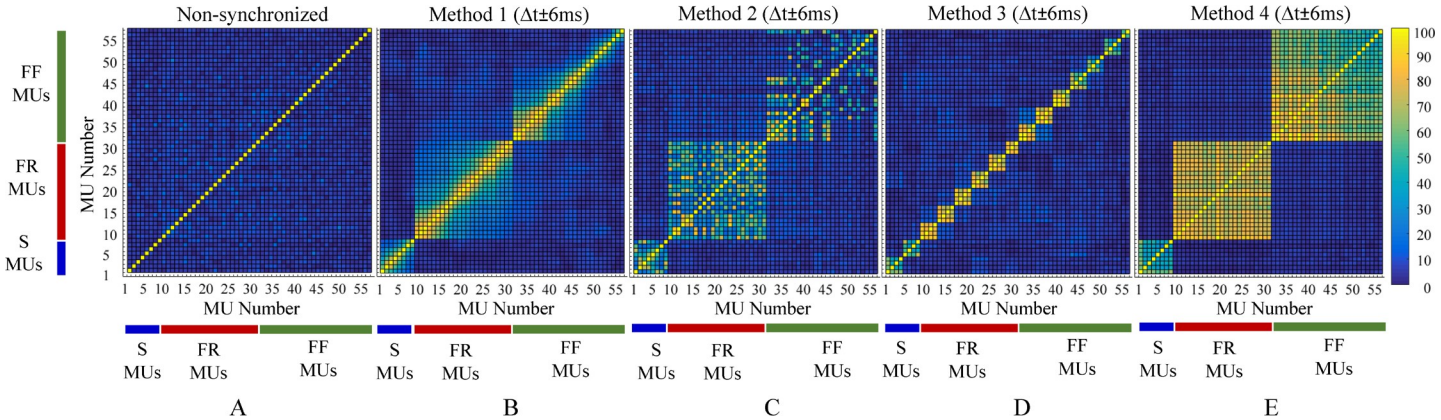

Fig 5. The correlation coefficients (*corMU*) between all pairs of 57 MU firing patterns for the *NS* model and for the four methods of MU synchronization using Δ*t* ± 6 ms. The color map represents ***corMU*** values in the range of 0% to 100% calculated within the square grid (57 × 57) of sequential MU numbers from 1 to 57. The diagonal elements of the color map correspond to a 100% correlation between the firing pulses of identical MUs.

https://doi.org/10.1371/journal.pcbi.1008282.g005

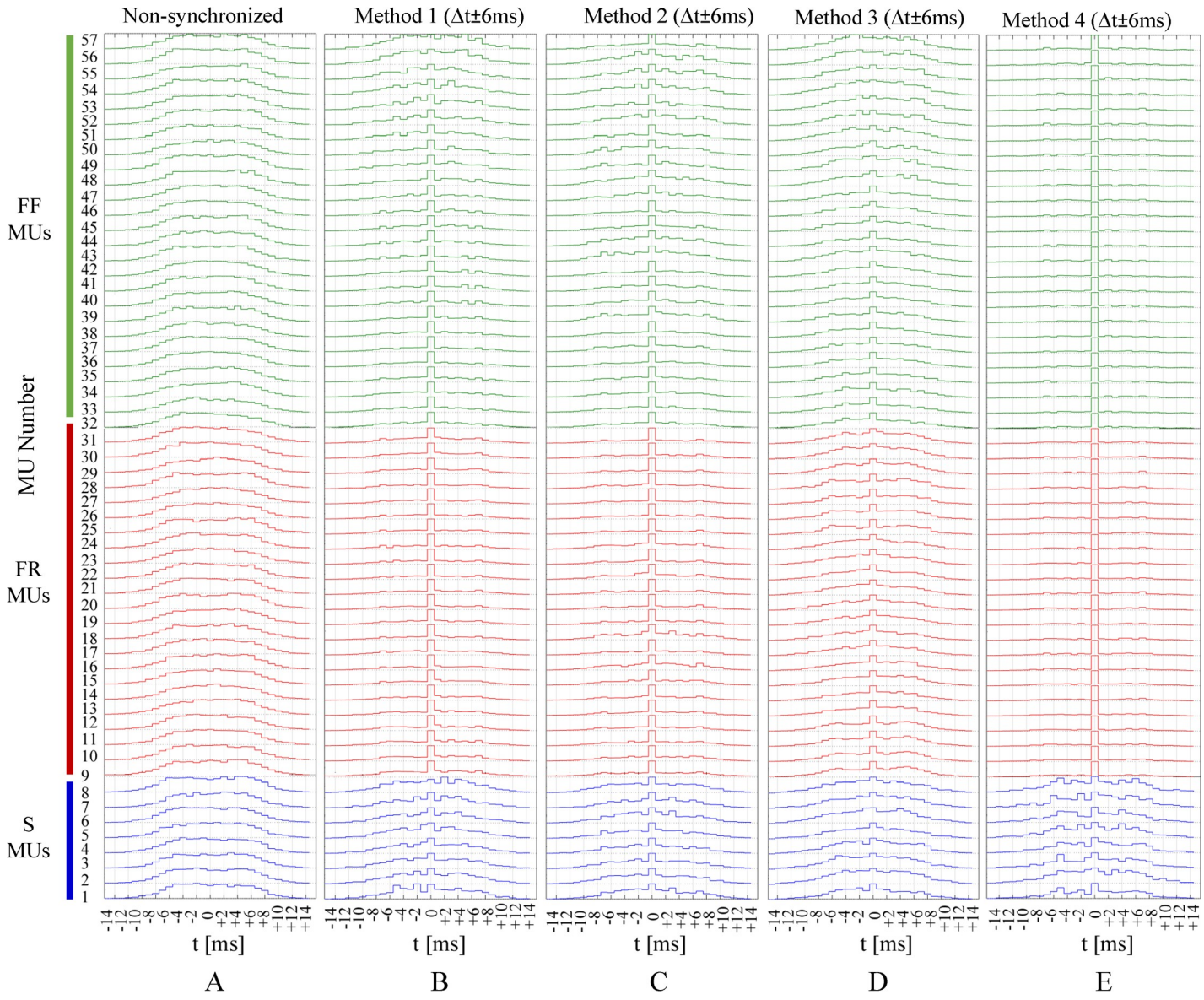

Fig 6. Cross interval histograms of all 57 MU firing patterns for the *NS* basic model and the four methods of MUs' synchronization using Δ*t* ± 6 ms. The cross-interval histograms are depicted with maximal bin normalization, considering a bins width of 1 ms within a bin interval of ± 15 ms. The amplitude of the central bin, presenting a minimal cross-interval difference of ± 0.5 ms, is proportional to the derived index of synchronization (***CISI***).

https://doi.org/10.1371/journal.pcbi.1008282.g006

Stronger synchronization of MU firings in different synchronization scenarios

The aforementioned 57 MU firing patterns of the basic muscle model were modified according to 12 synchronization scenarios, i.e., four synchronization concepts (Methods 1–4) each applied within three synchronization time intervals (Δ*t* = ± 2, ± 4, and ± 6 ms). The resultant average levels of synchronization between patterns of MUs of the same physiological type and within the whole muscle are estimated in Table 2. In all cases, certain increments of both indices for the level of MU synchronization (*corMU* and *CISI*) were assessed in comparison with their estimation for the basic *NS* model in the first row of Table 2. Therefore, it may be concluded that the simulation design achieved the general goal for inducing stronger

synchronization between MU firings. More details on the observed MU synchronizations related to the computation of *corMU* and *CISI* are presented below.

- *corMU*: Different effects of the synchronization induced by Methods 1 through 4 could be tracked well on the *corMU* color map (Fig 5B, 5C, 5D and 5E), seen as clusters with strong correlations (*corMU* is from 30% to 100%). These clusters have different two-dimensional space distributions of the entries with maximal correlation, corresponding to the different concepts for synchronization of MU pairs in Methods 1 through 4, as follows:
  - *Method 1*: The synchronization between neighboring MUs is seen in Fig 5B as maximal correlations around the main diagonal (identical MUs and their closer neighbors) and a trend of gradually decreasing correlations moving away from that diagonal (MU pairs with far neighborhood). Three clusters with *corMU* gradient can be identified in Fig 5B as a result of synchronization within MUs of the same physiological type (S–S, FR–FR, FF–FF). Within these clusters, the maximal correlation (mean value ± standard deviation) is observed for FR MUs (38.4% ± 21.1%), S MUs (37.2% ± 19.5%), and minimally for FF MUs (22.3% ± 22.4%), considering the setting with a maximal synchronization interval $\Delta t = \pm 6$ ms (Table 2). This means up to 30% increase in the correlation coefficients within MU groups, as compared with in the basic *NS* model.
  - *Method 2*: The synchronization was applied to not ordered MU pairs within the same physiological type; therefore, the *corMU* color map in Fig 5C appears with a non ordered colorful distribution with strong correlations between various MU pairs, forming three clusters within MUs from the same physiological type (S–S, FR–FR, FF–FF). Within these clusters, maximal correlation (mean value ± standard deviation) was observed for FR MUs (39.7% ± 21.5%), S MUs (38.1% ± 19.7%), and minimally for FF MUs (20.2% ± 21.9%), considering the setting with a maximal synchronization interval $\Delta t = \pm 6$ ms (Table 2). We note that the reported average *corMU* values in Method 2 are very similar to those in Method 1. Considering that both methods had a common concept for MU synchronization in pairs, we could deduce that the synchronization concept and not the order of MU recruitment can help in increasing the synchronization index by up to 30%, although the effect on the output force is expected to be different.
  - *Method 3*: The synchronization between unique groups of four neighboring MUs is seen in Fig 5D as maximal correlations in clusters with (4 × 4) entries, distributed around the main diagonal (including the identical MU pair and its three closest neighbors). There are two exceptions with smaller clusters, including 3 × 3 entries (MU numbers 29, 30, 31) and 2 × 2 entries (MU numbers 56, 57), which exactly correspond to the methodological constraints. Considering all MUs within the same physiological type, the maximal correlation (mean value ± standard deviation) is estimated for S MUs (15.7% ± 14.8%), FR MUs (13.5% ± 16.2%), and minimally for FF MUs (9.9% ± 13.9%) in the setting with a maximal synchronization interval $\Delta t = \pm 6$ ms (Table 2). This result yields an increment of 6% to 18% of *corMU* after Method 3 synchronization relative to the basic *NS* model. In general, Method 3 induces a smaller level of synchronization than Methods 1 and 2, which can be deduced from the larger size of the dark blue color area with uncorrelated MU pairs found in Fig 5D as compared with in Fig 5B and 5C.
  - *Method 4*: The concept for synchronization of all MUs within the same physiological type to only one reference MU resulted in MU clusters with very high pairwise correlations, enclosing all MUs in the respective physiological type (S–S, FR–FR, FF–FF). Within these clusters, the maximal correlation (mean value ± standard deviation) was observed for FR

MUs (74.6% ± 6.9%), FF MUs (62.8% ± 13.1%), and minimally for S MUs (42.6% ± 10.9%) in the setting with a maximal synchronization interval $\Delta t = \pm 6$ ms (Table 2). This result yields an increment from 37% to 67% of the correlations within MU groups relative to the basic *NS* model and can be denoted as the maximal synchronization level simulated in this study.

- *CISI*: The effect of synchronization induced by Methods 1 through 4 could be identified in the cross-interval histograms (Fig 6B, 6C, 6D and 6E) by the prominent peak in the central bin (± 0.5 ms). The larger is amplitude deviation from the uniform distribution in other bins, the higher the probability for synchronization of the respective MU to the firing pulses of other MUs. Different synchronization methods produce different amplitudes in the central bin, estimated by *CISI* in Table 2. Comparing the *CISI* values of all methods estimated with maximal synchronization interval $\Delta t = \pm 6$ ms, we could deduce the following:
  - The lowest *CISI* mean value was found for S MUs (from 8.2% in Method 3 to 10.3% in Method 2, with the latter being up to 4.5% above the basic *NS* model).
  - The largest *CISI* mean value was found for both FF MUs (from 9% in Method 3 to 31.6% in Method 4) and FR MUs (from 9.7% in Method 3 to 32.1% in Method 4). Thus, the best synchronization of Method 4 achieved up to a 25.9% greater *CISI* value as compared with the basic *NS* model.

Additionally, Fig 7A was designed to show the effect of widening the time window for synchronization ($\Delta t = \pm 2, \pm 4$, and ± 6 ms) on the relative *CISI* change (ratio of synchronized vs. *NS* value). It shows that, generally, $\Delta t = \pm 2$ ms leads to weak synchronization and slight increases in *CISI* by about 1.1 times (Methods 1–3) and 1.8 times (Method 4); $\Delta t = \pm 4$ ms lead to maximal synchronization that is still less than two times (Methods 1–3) but about three times (Method 4); and $\Delta t = \pm 6$ ms produced the maximal synchronization with notable *CISI* increment increases by up to three times (Methods 1 and 2) and up to five times (Method 4).

Maximal effect of MU synchronization on the force parameters

The forces produced by the muscle and different MU types before and after the application of different synchronization scenarios were estimated for a two-second period during the muscle steady state and the defined six basic force parameters (*meanF*, *rmsF*, *rangeF*, *maxF*, *VAF and meanfreq*) are presented in Table 3. For comprehension purposes, the representation of those parameters on the force signals and their PSD (power spectral density), is additionally illustrated in Fig 8. The comparison of the *NS* excitation to those achieved with different synchronization methods (Methods 1–4) is presented below.

- *Force mean value*: The synchronization had no effect on *meanF* parameter, which accounted the value of the mean force. It showed a negligible change ($\leq$ 12 mN) before and, after the synchronization was applied, i.e., for the muscle force, *meanF* was varying from 4052 mN (*NS*) to a maximum of 4064 mN (Method 4, $\Delta t = \pm 6$ ms) (Table 3). This can be also tracked in Fig 8A, which presents no visible difference in the baseline value (red solid horizontal line) when comparing all forces placed in a row.
- *Force RMS value*: The synchronization had an important effect on the force variance, increasing the *rmsF* value by more than 50 mN. It could become as high as 129 mN for the muscle force (Method 4, $\Delta t = \pm 6$ ms), considering its baseline *NS* value of 73.5 mN (Table 3). Additionally, Fig 7B is provided to show the relative *rmsF* change as a ratio of synchronized vs. *NS* value. Specifically, it shows that the maximal *rmsF* increment (about two

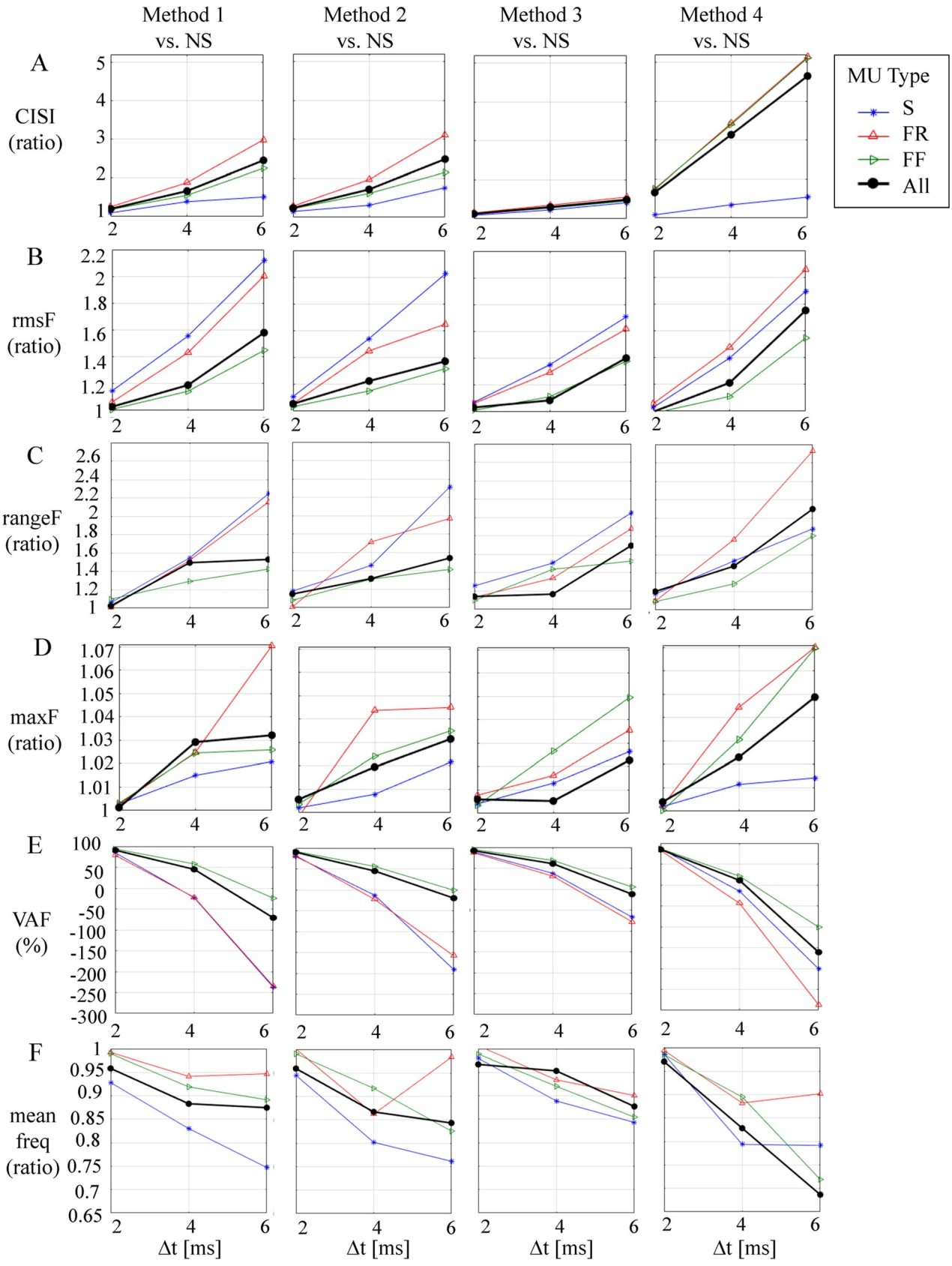
Method 1 vs. NS
Method 2 vs. NS
Method 3 vs. NS
Method 4 vs. NS
A
CISI (ratio)
B
rmsF (ratio)
C
rangeF (ratio)
D
maxF (ratio)
E
VAF (%)
F
mean freq (ratio)
MU Type
S
FR
FF
All
Δt [ms]

Fig 7. Effects of widening the time window for synchronization (Δt = ± 2, ± 4, and ± 6 ms) on an increment of the cross-interval synchronization index of MU pulses (*CISI* in panel A), the force root-mean squared value (*rmsF* in panel B), the force range (*rangeF* in panel C), the maximum force (maxF in panel D), as well as the force parameter *VAF* (in panel E) and the force mean spectral frequency (*meanfreq* in panel F), presented as the ratio of values calculated for each method of synchronization (Methods 1–4) vs. the *NS* basic model.

https://doi.org/10.1371/journal.pcbi.1008282.g007

times) could be achieved for the forces of two types of MUs (S, FR) following synchronization with Methods 1, 2, and 4, Δt = ± 6 ms. Considering the whole muscle, the observed maximal increment of *rmsF* was about 1.8 times, achieved using Method 4, Δt = ± 6 ms.

- *Force min–max range*: The synchronization had an important effect on the force variance, increasing the *rangeF* value by about 450 mN. It grew from 405 mN (*NS*) up to 850 mN for the muscle force after synchronization with Method 4, Δt = ± 6 ms (Table 3). The *rangeF* ratio (synchronized vs. *NS* value) in Fig 7C shows that the largest *rangeF* increment (two to 2.6 times) was achieved for the forces of two types of MUs (S, FR) after synchronization with Methods 1, 2 and 4, Δt = ± 6 ms. Considering the whole muscle, the observed maximal increment of *rangeF* (about 2.1 times) was with Method 4, Δt = ± 6 ms. Although the observations concerning *rangeF* are similar to those of *rmsF* as was noted above, the relative and absolute

Table 3. Estimation of the six force parameters *meanF*, *rmsF*, *rangeF*, *maxF*, *meanfreq* and *VAF* of different physiologicl types of MUs (S, FR, and FF) and the whole muscle, produced by the *NS* model and four methods for synchronization (Methods 1–4), within three time windows (± 2, ± 4, and ± 6 ms).

		S	FR	FF	muscle	S	FR	FF	muscle	S	FR	FF	muscle
		meanF **[mN]**				***rmsF*** **[mN]**				***rangeF*** **[mN]**			
NS		**385**	**1449**	**2219**	**4052**	**3.2**	**27.2**	**71.2**	**73.4**	**16.8**	**146**	**395**	**405**
Method 1	**±2ms**	385	1449	2217	4051	3.7	28.9	71.8	75.4	17.8	147	434	415
	±4ms	385	1449	2218	4052	5.0	38.9	81.4	87.2	26.0	222	511	606
	±6ms	385	1453	2228	4066	6.9	54.5	103	116	37.7	314	564	620
Method 2	**±2ms**	385	1449	2218	4052	3.6	28.7	73.6	77.4	19.8	147	427	465
	±4ms	385	1449	2226	4059	5.0	39.4	81.9	89.9	24.5	250	518	533
	±6ms	385	1450	2226	4061	6.5	44.9	93.8	101	38.8	287	560	624
Method 3	**±2ms**	385	1448	2218	4051	3.5	28.9	72.0	75.8	21.1	165	434	462
	±4ms	385	1448	2216	4049	4.4	35.2	79.2	79.7	25.3	195	568	472
	±6ms	385	1447	2223	4057	5.5	44.0	98.1	103	34.4	274	603	687
Method 4	**±2ms**	385	1449	2218	4052	3.3	28.8	70.1	73.1	19.7	160	431	487
	±4ms	385	1451	2217	4051	4.5	40.1	79.1	88.9	25.7	257	508	599
	±6ms	385	1458	2224	4064	6.1	56.0	110	129	31.6	397	714	850
		maxF **[mN]**				***mean freq*** **[Hz]**				***VAF*** **[%]**			
NS		**393**	**1519**	**2398**	**4234**	**13.6**	**24.0**	**36.1**	**35.6**	**100**	**100**	**100**	**100**
Method 1	**±2ms**	395	1523	2406	4239	12.6	23.8	35.7	34.1	85	79	94	91
	±4ms	399	1557	2457	4357	11.3	22.6	33.1	31.5	-23	-22	58	45
	±6ms	402	1627	2460	4370	10.2	22.7	32.2	31.5	-237	-235	-24	-71
Method 2	**±2ms**	394	1517	2407	4258	12.9	24.0	35.7	34.2	80	82	92	90
	±4ms	397	1586	2456	4316	10.9	20.7	33.1	30.9	-13	-23	56	45
	±6ms	402	1588	2482	4367	10.4	23.6	29.8	30.0	-191	-158	-1.1	-20
Method 3	**±2ms**	395	1531	2407	4259	13.3	24.1	35.7	34.4	89	87	95	92
	±4ms	399	1544	2462	4256	12.1	22.4	33.2	33.9	38	31	69	61
	±6ms	404	1574	2517	4330	11.5	21.6	30.8	31.2	-67	-78	5.2	-12
Method 4	**±2ms**	394	1523	2399	4250	13.4	23.8	35.5	34.6	87	83	87	85
	±4ms	398	1587	2472	4331	10.8	21.2	32.3	29.5	-15	-44	21	11
	±6ms	399	1626	2565	4440	10.8	21.6	25.9	24.4	-201	-287	-101	-161

https://doi.org/10.1371/journal.pcbi.1008282.t003

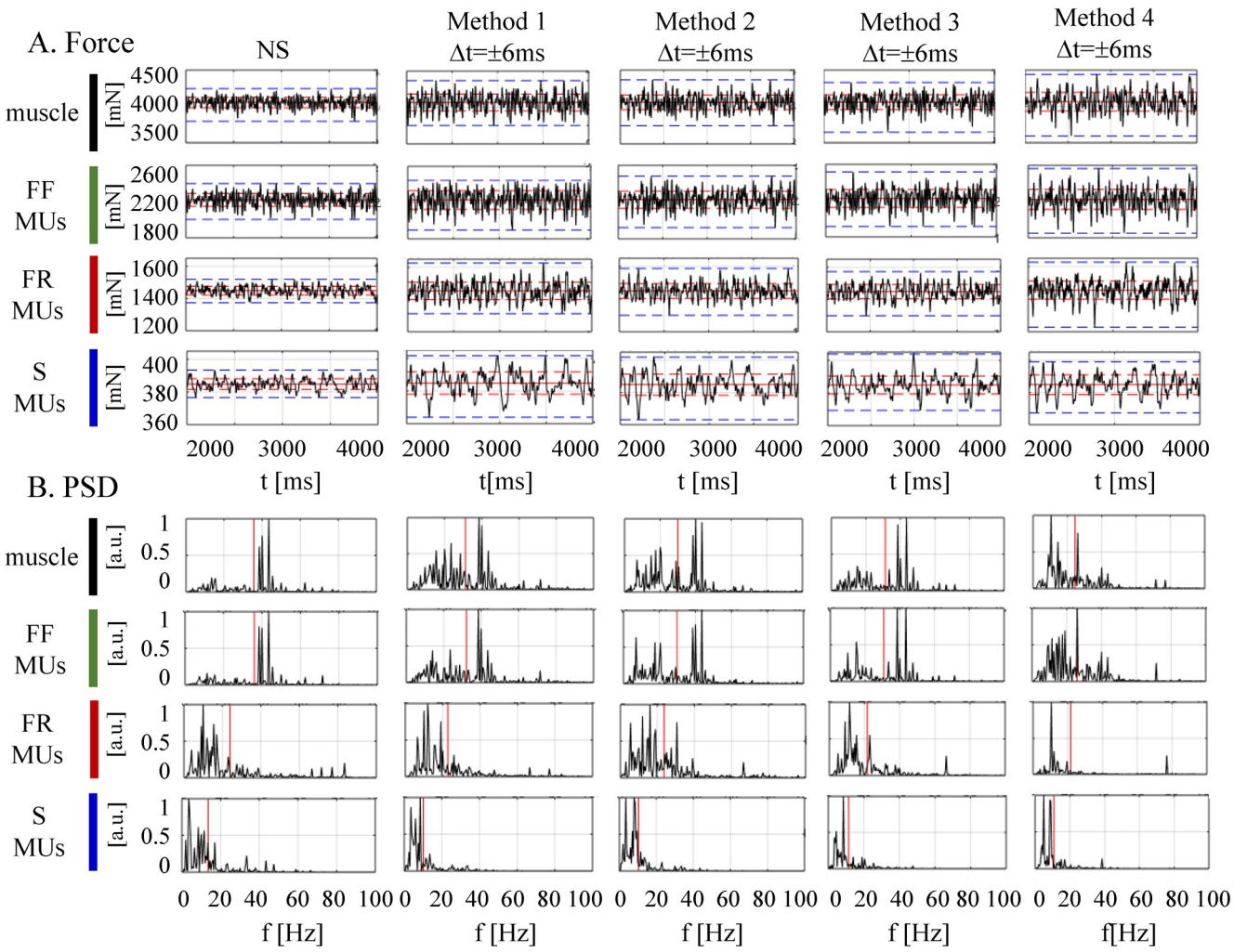

Fig 8. The forces (A) and respective power spectral densities–PSD—(B) calculated for the muscle and different MU types (S, FR, and FF) during the muscle steady state of the *NS* excitation and by using four methods of MU synchronization (Δ*t* ±6 ms). Values of different force parameters are indicated in each box of panel A as follows: the mean force by a red horizontal solid line, the force ***rms*** by a red horizontal dotted line, and the force range by a blue horizontal dotted line; meanwhile, the mean frequency is indicated in each box of panel B by a red vertical thick line.

https://doi.org/10.1371/journal.pcbi.1008282.g008

changes in *rangeF* values as an effect of synchronization were larger. This could also be visually confirmed by the force signals in Fig 8A (blue dotted lines show larger span than red dotted lines after synchronization, comparing all forces placed in a row).

- *Maximal force*: The synchronization had an important effect on increasing the *maxF* value by more than 205 mN, which could raise it from 4234 mN (*NS*) up to 4440 mN for the muscle force after synchronization with Method 4, Δ*t* = ± 6 ms (Table 3). The *maxF* ratio (synchronized vs. *NS* value) in Fig 7D shows that the largest *maxF* increment (up to 1.7 times) is achieved for the forces of two types of MUs (FR, FF) after synchronization with Method 4 or Method 1, Δ*t* = ± 6 ms. Considering the whole muscle, the observed maximal increment of *maxF* was about 1.5 times using Method 4, Δ*t* = ± 6 ms. This relative change of *maxF* was found to be smaller than the force amplitude variances estimated above by the other two force parameters (*rangeF* and *rmsF*). This could be explained by the fused nature of

maximum force, accumulating both the force mean and variance, the former shown above to be unaffected by synchronization.

- *VAF*: The synchronization had an important effect on the force variance estimated by *VAF*, which was decreasing from 100% (*NS*), greater than 80% (weak synchronization with $\Delta t = \pm$ 2 ms) to down below -200% (strong synchronization with Methods 1, 2 and 4, $\Delta t = \pm$ 6 ms), as shown in Table 3 and Fig 7E. Negative values of *VAF* are not typical in literature, although Okada et al (2017) [40] reported that *VAF* decreased from positive to negative values when the analysis time window was widening. The negative *VAF* in our case was computed due to high variance of the force differences before and after synchronization, which was more than twice larger than the reference variance of the non-synchronized forces. This undoubtedly indicated that the synchronized forces had a very large variance, and they were completely non-synchronized with the forces of the non-synchronized model. Specifically, the synchronization of two types of MUs (S, FR) was noted as most influential on force *VAF* decrement (Table 3, Fig 7E), which corresponds to the above observations for largest *rmsF* values for the output forces of those types of MUs (Fig 7B).
- *Force mean spectral frequency*: In this context, the synchronization had an important effect—decreasing the *meanfreq* value by more than 10 Hz, which drops it from 35.6 Hz (*NS*) down to 24.4 Hz for the muscle force after synchronization with Method 4, $\Delta t = \pm$ 6 ms (Table 3). The *meanfreq* ratio (synchronized vs. *NS* value) in Fig 7F shows that the largest *meanfreq* drop (i.e., < 0.75 or $> 25\%$ vs. *NS*) could be achieved for the forces of two types of MUs (S, FF) after synchronization with Methods 1, 2 and 4, $\Delta t = \pm$ 6 ms. Considering the whole muscle, the observed maximum drop of *meanfreq* was about 30% (< 0.7 Hz) with Method 4, $\Delta t = \pm$ 6 ms. This can be observed in the *PSD* of Fig 8B (first row for the muscle force and second row for FF MU force) as a shift of the high-frequency components (predominantly around 40 Hz) in the *NS* spectrum to low-frequency components (10–25 Hz) in the spectrum for synchronization with Method 4, $\Delta t = \pm$ 6 ms.

It is worth to stress that unlike S or FR MUs, within FF MUs greater synchronization effects were revealed for the weaker subpopulation of units (FF32—FF44) than for the stronger ones (FF45-FF57) in three applied simulations methods (Method 1, 2, 4, Fig 5).

Correlation of the force variance and MU synchronization

The results presented in this section aim to answer the general question of whether the provided synchronization methods regularized by widening the time window for synchronization ($\Delta t = \pm$ 2, ± 4, and ± 6 ms) led to consistent increases in both the level of MU synchronization (*CISI*) and the induced changes in the force output. Thus, the force parameters, which were most closely correlated to the synchronization design in Methods 1 through 4, could be deduced. The results in Table 4 establish the correlations between the curves in Fig 7A for the level of MU synchronization in the function of Δt ($CISI = f(\Delta t)$) and each of the curves in Fig 7B, 7C, 7D and 7F for the trends of the six force parameters as a function of Δt (*meanF*, *rmsF*, *rangeF*, *maxF*, *VAF*, *meanfreq*). The correlations were estimated in the range [−1;+1], where +1 and −1 stand for strongly correlated curves that were directly or inversely proportional, respectively. The results show strong correlations of all parameters, which account for increasing the force variance while increasing the level of synchronization (i.e. *rmsF*, *rangeF*, *maxF* and *VAF* with an average correlation of about ± 0.97 in all types of MUs). The force mean spectral frequency was indeed inversely proportional to the synchronization level, with an average correlation coefficient of −0.89. The parameter related to the mean force (*meanF*) was the one least dependent on the synchronization, with an average correlation coefficient of 0.53.

Table 4. Correlation coefficients between *CISI* and the six force parameters *meanF*, *rmsF*, *rangeF*, *maxF*, *VAF* and *meanfreq*. The strength of the correlation is coded with a color gradient, highlighting the strong positive (> 0.8) (dense red) and strong negative (< −0.8) (dense blue) correlations.

Force	Method 1				Method 2				Method 3				Method 4			
parameters	S	FR	FF	all	S	FR	FF	all	S	FR	FF	all	S	FR	FF	all
meanF	-0.30	0.93	0.89	0.90	-0.36	0.88	0.88	0.90	0.13	0.70	0.57	0.57	-0.51	0.84	0.73	0.78
rmsF	0.96	1.00	0.99	0.99	0.98	0.96	1.00	0.99	0.99	0.98	0.94	0.91	0.98	0.99	0.92	0.95
rangeF	0.95	0.99	0.97	0.88	1.00	0.94	0.97	0.99	1.00	0.96	0.97	0.92	1.00	0.99	0.97	0.99
maxF	1.00	0.99	0.87	0.89	0.99	0.86	0.98	0.99	1.00	0.98	0.98	0.90	0.99	0.99	0.98	0.99
VAF	-0.92	-1.00	-0.99	-0.99	-0.99	-1.00	-0.99	-1.00	-0.98	-0.96	-0.95	-0.96	-0.97	-0.97	-0.98	-0.97
meanfreq	-0.99	-0.82	-0.94	-0.88	-0.90	-0.21	-0.99	-0.93	-0.98	-0.95	-0.98	-0.96	-0.94	-0.86	-0.97	-1.00

https://doi.org/10.1371/journal.pcbi.1008282.t004

Discussion

There are two different approaches one could use to investigate the synchrony between different MUs and its influence on the developed muscle force. The first one involves assessing experimental recordings of electromyographic signals using needle or surface electrodes and decomposing these signals into individual action potentials [4,41–44]. However, the disadvantages of this approach include that only a portion of the active MUs is recorded, it is not possible to distinguish fast from slow MUs and the measured muscle force reflects the force of all active MUs, and even MUs of other muscles. The second method is based on pure modeling, wherein models of the muscle are composed using different MUs [22,32]. These models are based on the Fuglevand et al. approach [31] which contain 120 MUs. However, these authors did not divide MUs into different types (S, FR, and FF). Moreover, the function used for describing the twitch was based only on two parameters: force amplitude and contraction time. The model used in the current paper, is constructed based on experimental data concerning MU twitch and tetanus properties as well as motoneuronal excitability, and has been fully described previously [34]. Here, the experimentally measured twitches are modeled by a six-parameter function and the summation of the twitches into tetanus is established by an experimentally verified mathematical algorithm. In the adopted basic model, it was proven that the firing of all MUs is asynchronous. Then, synchronization was imposed in this basic MU firing arrangement, changing the pattern of pulses of MUs during the steady state of the muscle force using several simulated situations (i.e., four modes of synchronization with the three time windows ± 2, ± 4, and ± 6 ms). In this way, broad investigation of the influence of the synchrony of the three types of the MUs on the developed muscle force and cumulative forces of MUs from the three groups could be performed. The results based on the two used coefficients *corMU* and *CISI* showed that the range, the maximum, and the root-mean-square of the forces rose with increased synchronization, while the mean forces remained nearly unchanged. This increase was stronger for fast MUs; notably, these units are mostly responsible for the force instability (muscle tremor) in the context of moderate or strong muscle contractions, wherein fast MUs are recruited into activity.

Models of MU synchronization

To increase the degree of synchronization and to analyze its effects on the muscle and MU forces, we considered the synchronization of pulses of pairs of MUs in the time windows ± 2, ± 4, and ± 6 ms. It is known that synchronization is an effect of a common excitatory input to several motoneurons and that synchronic excitatory postsynaptic potentials (EPSPs) evoked in several motoneurons increase the probability of the simultaneous occurrence of their action potentials [45]. The size of the time windows is related to the duration of EPSPs in rat

motoneurons, lasting several milliseconds, with an increasing phase often remaining below 2 ms (for example, for Ia monosynaptic EPSPs, see **Fig 1** in Seburn and Cope [46]). Additionally, the applied method resulted in a narrow peak in the cross-interval histogram (Fig 6), similar to that reported for human muscles by De Luca et al. [4], as is typical for short-term synchronization (i.e., the peak centered about zero-time delay 0.5 ± 2.9 ms) and with an average width of 4.5 ± 2.5 ms. For all four proposed modes of synchronization used in the present study, the same range of time windows was applied. The largest (± 6 ms) time window increased the *CISI* by about 1.5 times for Method 1, about 2.5 times for Methods 2 and 3, and more than three times for Method 4 (see Table 2). The range of differences in the obtained synchronization is similar to that of differences in the *CISI* reported for trained and nontrained subjects (more than two times higher in weightlifters), changes resulting from conditioning exercise (about 2.5 times higher after the exercise), and those between dominant and nondominant hands (1.6 times higher in the no dominant hand) [43].

The proposed method of inducing synchronization within time windows Δt of variable duration appeared to be an efficient tool in the four tested simulations. For all four methods of synchronization, values of the investigated parameters, which account for the force variance (*rmsF*, *rangeF*, *maxF* and *VAF)* which characterized amplified force oscillations, changed along with increases in the time window Δt, i.e., when the synchronization degree was augmented (Fig 7). Notably, this change appeared strongest with Method 4 and weakest with Method 3. Meanwhile, the highest value of *corMU* (74.6) was achieved for $\Delta t = \pm 6$ ms for FR MUs (Table 2). Moreover, except for in Method 3, the highest values of *corMU* were observed for FR MUs (Table 2). This observation is surprising in light of previous physiological experiments concerning force decreases/increases resulting from the prolongation/shortening of one IPI during the unfused tetanic contraction ascertained using MUs of the rat medial gastrocnemius muscle [29]. Namely, relative force fluctuations noted for FF and FR MUs were similar and one could expect no differences to exist between these two types of fast MUs in the present simulation study. This methodological approach resulted in the highest synchronization for Method 4 and is reflected by the parameters *corMU* and *CISI* in Table 2. It should be stressed that the four methods led to similar effects on muscle force—that is, greater maximal force and higher fluctuations around a mean force—and these increases concerned all three types of MUs, although it should be stressed that this result was obtained for the maximum excitation signal, i.e., a simulation of a very strong contraction, when all MUs were active.

The induced synchronization patterns have random character. First of all, impulses of each individual MU, firing with a given mean frequency, were distributed randomly by an algorithm changing successive IPIs. Second, synchronization was induced only when impulses of two MUs occurred in a close time interval (of 2, of 4 or of 6 ms), which was also a random situation since the time with which the impulse is shifted is random. The synchronization procedure modified the distribution of IPIs for all MUs included in the model and shapes of histograms (S1 Fig in the supplementary material) for non-synchronized and synchronized IPIs (Methods 1–4) were similar to those reported by authors studying MU firing rates in human muscles during voluntary activity [47,48]. Nevertheless, the increased minimum to maximum range of IPIs observed in the histograms in result of four applied methods of synchronization turns our attention to a significance of rate coding. In a recent study on insects Putney et al. (2019) [49] reveled that timing of impulses between motoneuron discharge patterns plays a higher role than a number of pulses, but it is well known that changes in IPIs are crucial for the force development also in the mammalian (cat and rat) muscles [29,30,35,50,51,52].

We decided to induce synchronization within each type of MUs (S, FR or FF, but not randomly between all types of MUs), which corresponded to the primary goal of the study

concerning the role of synchronization of particular types of MUs. Moreover, assumptions of the common-drive hypothesis regarding common input to numerous motoneurons in a pool innervating a muscle have some limitations, and there may be several basic patterns of synaptic input organization to motoneurones within a given MU pool. Both peripheral and descending inputs to slow and fast motoneurons differ with respect to latencies or amplitudes of postsynaptic potentials. For example, monosynaptic EPSPs from muscle spindles are the largest in type S MUs, smaller in type FR, and smallest in type FF units [53], disynaptic IPSPs facilitated by rubrospinal volleys are the highest in slow and lowest in fast MUs [54], slow and fast forelimb motoneurons receive different inputs from propriospinal neurons conveying pyramidal commands [55]. All these observations indicate that groups of motoneurons of MUs of each type form specific subpopulations within a motor nucleus.

Effects of synchronization on MU and muscle forces

The influence of the increasing synchronization level on the mean as well as on the maximum force of particular MU types and of the whole muscle was, in general, very weak (i.e., the maximum force increased by up to 5% for the whole muscle and up to 7% for FF MUs), regardless of the synchronization method applied in the model. This confirms the results of previous studies, which also demonstrated that the magnitude of force output and the average force of the muscle were not altered considerably due to synchronization [22,43]. However, an increase in the synchronization time window from ± 2 to ± 6 ms in all cases correlated with a rise in the force of each MU type, with the change being the greatest for synchronization using Methods 1 and 4. Moreover, the present study has revealed certain differences between MU types. Not only did the absolute force increase but also the relative force increased after synchronization; further, they were always the highest for fast MUs (FF and FR) and the lowest for slow MUs. This also confirms previous observations that synchronization may be beneficial during the performance of contractions where rapid force development is required, for which fast MUs should be recruited [18].

On the other hand, it was already mentioned that a muscle can produce smooth contractions due to asynchronous discharges of motor neurons [18,24] and that synchronization increases the variability in the muscle force [22]. Indeed, simulated contractions in our model have confirmed that synchronization substantially influences the range of force oscillations during the steady state of the muscle contraction and the min–max range of modeled forces gradually rose with the increase in the time window for synchronization in each method. This can be partly explained by previous computer simulations indicating that synchronization leads to an increase in the estimated twitch force and to a decrease in the estimated contraction time of an MU [27]. Obviously, absolute values of the min–max range of the force were the lowest for the weakest S MUs, but the ratio of parameters accounting for the force variance (*rmsF*, *rangeF*, *VAF*) between synchronized and *NS* models was the highest for S MUs for all methods—except Method 4, in which MUs of the same type were synchronized according to the first MU in the group (see Fig 7B, 7C and 7F).

A 100% excitation signal (corresponding to a very strong muscle contraction) used in this model was applied to ensure activation of all MU types, which helped us to elucidate the contributions of the three types of MUs to muscle tremor, which are dependent on the force level [56]. According to the size principle, at a lower excitation signal, a contribution of high-threshold fast MUs (especially those of the FF type) to the force development would be smaller or recruitment would be restricted to low-threshold (S or FR) MUs. The lowest relative force oscillations were noted in FF MUs for all methods of synchronization (Fig 7B and 7E). This observation indicates that slow MUs have the strongest and FF MUs have the weakest relative

influence, respectively, on force fluctuations described as muscle tremor and thus partly explains why tremor is best visible during weak contractions, when predominantly slow MUs are recruited.

Surprisingly, the model indicated that weaker and stronger FF MUs revealed different synchronization effects (Fig 5). The model is based on data concerning contractile properties of a set of MUs studied in electrophysiological experiments, selected from a large population of units to form a group of MUs reflecting a real number and proportion of MU types (S, FR and FF) in the medial gastrocnemius muscle. Moreover, they were selected to represent mean values of their contractile properties as close as possible to those observed in the whole population. MUs are recruited in the model in order of the increase in the input to motoneurons, and according to the size principle, i.e. from the weakest to the strongest MU within each type. As indicated in Table 1, FF MUs are ordered according to their increasing twitch force and a half of weaker ones (FF32—FF44) have somewhat different properties than the stronger ones (FF45—FF57). Namely, the weaker FF MUs have shorter twitch time parameters than the stronger FF units (the contraction time 13.4±1.7 *vs* 14.2±1.4 ms, the half-relaxation time 25.4 ±4.6 *vs* 27.8±4.5 ms), while their firing rates predicted by the model are higher (57.9±14.1 *vs* 48.0±9.6 ms, respectively), because the firing rate is dependent on the twitch contraction time [34]. Lower firing rate decreases a number of action potentials in the studied time window and most probably provides an explanation of the observed sub-grouping observed in Fig 5. Nevertheless, a question whether stronger FF MUs (those with the highest recruitment threshold) reveal weaker synchronization is open and needs to be studied in separate physiological experiments.

The influence of synchronization on the spectral frequency of the muscle force

To our knowledge, the parameter *meanfreq* of the force has not been analyzed in muscle modeling in connection with the synchronization of MU firing to date. It should be noted, however, that the power spectral analysis of tremor in the first dorsal interosseous muscle revealed three frequency peaks occurring at around 10 Hz, 20 Hz, and 40 Hz [25], which correspond to our findings concerning the mean spectral frequencies of S, FR, and FF MUs, respectively (Table 3). McAuley et al. [25] concluded that their results reflected the synchronization of MUs at frequencies determined by oscillations within the central nervous system; however, our findings suggest that the force oscillations related to three types of MUs likely contribute to those frequency peaks.

A decrease in the *meanfreq* was observed in parallel with an increase in the degree of synchronization in all four applied methods. It should be stressed that the mean firing frequencies of all MUs remained unchanged during simulations, due to a constant number of pulses in the analyzed time window (2000 ms). A decrease in force spectral frequencies paired with the occurrence of slower force oscillations. This observation at increased synchronization levels indicates that the force-frequency spectrum depends upon the temporal distribution rather than on the mean firing frequencies of MUs and this conclusion concerns all three types of MUs, despite considerable differences in the *meanfreq* between S, FR, and FF MUs. The decrease in the *meanfreq* could not be linked to muscle fatigue, which was not modeled, and should instead be connected with processes of summation of twitches into tetanic contractions.

McAuley and Marsden [57] in their review argued that the physiological tremor in humans is likely of multifactorial origin, with contributions from the 10-Hz range of oscillatory activity of the central nervous system, MU discharge frequencies, reflex loop resonances, and

mechanical resonances. However, it must be emphasized that the present results were obtained using the model of a rat muscle, so it is risky to directly compare the frequencies related to different types of MUs collected herein to human data, most of all because rat MUs demonstrate considerably faster contractions and have higher discharge frequencies.

Significance of the results

This is the first study on functional consequences of increasing synchronization in MUs' firing related to the MUs' type. It should be stressed that data concerning the MUs' synchronization have been obtained so far predominantly in human experiments from EMG recordings from a voluntary active muscles, subsequently decomposed into trains of action potentials of MUs. It was found that the synchronization varied across different skeletal muscles [3,15], and increased as an effect of training [18,20,22] or fatigue [23]. It is well known that a certain proportion of different types of MUs is a characteristic feature of a given muscle (which can be composed predominantly of fast or slow MUs) [58,59], which is not permanent during altered motor activity, e.g. the endurance training can evoke adaptation in contractile properties mainly in FR MUs [60], whereas weight-lifting training can modify properties of FF MUs, as well [61]. On the other hand, development of fatigue is predominantly an effect of activity of FF MUs which have low fatigue index [59]. Therefore, the present observations made for separate MU types contribute to better understanding of consequences of MU synchronization in muscles which are different with respect to the MU content and activity levels.

Limitations of the study

The synchronization was studied within a limited interval of 2000 ms, including limited MU stimuli. Their average number was 100 (S MUs), 111 (FF MUs) and 140 (FR MUs) defining an average influence of the synchronization of a single pulse in the range from 0.7% to 1%. Although our analysis of synchronization did not account on this value, it might indirectly determine the resolution for computation of the correlation coefficient and *CISI*. More detailed analysis of intervals would improve the resolution; however, it is unlikely to change the observed global results, which revealed differences in presence and absence of synchronization much above 1% (Table 2).

It is assumed in the applied model that forces of all co-active MUs reveal algebraic, linear summation, and this is a simplification for several reasons. First, we know that in the modeled muscle (medial gastrocnemius) processes of summation of MUs forces are not linear, and most probably dependent on interactions between co-active MUs, and effects of summation of MU forces progressively decrease with the increased number of active units [62]. Second, the force production in a muscle depends on the muscle length (stretch) [63]. In the present paper we have used for modeling twitch properties obtained under isometric conditions, and therefore the presented results should be considered as modeling of the force produced during contractions of a muscle kept at a constant length. Third, in the present model MUs are not positioned within the muscle, and one should be aware that the interrelationships between muscle fibers of co-active MUs influence the cumulative force, and overlapping of MU territories most likely negatively influence the muscle force output [62]. A problem of interrelationships between neighboring MUs deserves to be modeled, although till now we have a limited input data to propose a reliable model.

Conclusion

The present study revealed that, regardless of the method used for the synchronization of MU firings, the increase in the synchronization index had a negligible effect on the mean force of

the developed contractions yet influenced muscle tremor by increasing force oscillations and further highlighted that these results were observed for all three types of MUs. A parallel decrease in the mean spectral frequency of the force indicated that, in the synchronized models, the force oscillations were slower despite higher magnitudes. The synchronization of fast MUs led to higher increases in the range of the force variability and the force root-mean-square in comparison with that of slow MUs. On the other hand, relative changes in the latter parameters in the synchronized simulations were the highest for slow MUs, indicating their significant contribution to muscle tremor, especially during weak contractions.

Supporting information

S1 Data. Supplementary material. Firing patterns for all 57 MUs when simulating basic (*NS*) model. These data are used for plotting Fig 2.
(XLS)

S2 Data. Supplementary material. Forces of whole muscle, group of S, FR and FF MUs calculated using 100% excitation signal for the basic model. These data are used for plotting Fig 1B.
(XLS)

S1 Fig. Supplementary material. Normalized histograms of inter pulse intervals of 57 motor units (MUs) of a rat muscle gastrocnemius model, including: 8 slow (S) MUs, 23 fast resistant to fatigue (FR) MUs, and 26 fast fatigable (FF) MUs.
(DOCX)

Acknowledgments

The study was supported by a bilateral agreement between the Bulgarian Academy of Sciences and the Polish Academy of Sciences.

Author Contributions

Conceptualization: Rositsa Raikova, Vessela Krasteva, Piotr Krutki, Jan Celichowski.

Data curation: Rositsa Raikova, Vessela Krasteva.

Formal analysis: Rositsa Raikova, Vessela Krasteva, Piotr Krutki, Jan Celichowski.

Funding acquisition: Jan Celichowski.

Investigation: Rositsa Raikova, Vessela Krasteva, Piotr Krutki, Hanna Drzymała-Celichowska, Katarzyna Kryściak, Jan Celichowski.

Methodology: Rositsa Raikova, Vessela Krasteva, Piotr Krutki, Katarzyna Kryściak, Jan Celichowski.

Resources: Jan Celichowski.

Software: Rositsa Raikova, Vessela Krasteva.

Validation: Rositsa Raikova, Vessela Krasteva, Piotr Krutki.

Visualization: Rositsa Raikova, Vessela Krasteva.

Writing – original draft: Rositsa Raikova, Vessela Krasteva, Piotr Krutki, Hanna Drzymała-Celichowska, Katarzyna Kryściak, Jan Celichowski.

Writing – review & editing: Rositsa Raikova, Vessela Krasteva, Piotr Krutki, Hanna Drzymała-Celichowska, Katarzyna Kryściak, Jan Celichowski.

References

1. Datta AK, Stephens JA. Synchronization of motor unit activity during voluntary contraction in man. J Physiol. 1990; 422:397–419. https://doi.org/10.1113/jphysiol.1990.sp017991 PMID: 2352185
2. Kutch JJ, Suresh NL, Bloch AM, Rymer WZ. Analysis of the effects of firing rate and synchronization on spike-triggered averaging of multidirectional motor unit torque. J Comput Neurosci. 2007; 22(3):347–361. https://doi.org/10.1007/s10827-007-0023-0 PMID: 17377834
3. Keen DA, Chou LW, Nordstrom MA, Fuglevand AJ. Short-term synchrony in diverse motor nuclei presumed to receive different extents of direct cortical input. J Neurophysiol. 2012; 108(12):3264–3275. https://doi.org/10.1152/jn.01154.2011 PMID: 23019009
4. De Luca CJ, Roy AM, Erim Z. Synchronization of motor-unit firings in several human muscles. J Neurophysiol. 1993; 70(5):2010–2023. https://doi.org/10.1152/jn.1993.70.5.2010 PMID: 8294967
5. Kirkwood PA, Sears TA, Stagg D, Westgaard RH. The spatial distribution of synchronization of intercostal motoneurones in the cat. J Physiol. 1982; 327:137–155. https://doi.org/10.1113/jphysiol.1982.sp014224 PMID: 7120135
6. Schmied A, Ivarsson C, Fetz EE. Short-term synchronization of motor units in human extensor digitorum communis muscle: relation to contractile properties and voluntary control. Exp Brain Res. 1993; 97(1):159–172. https://doi.org/10.1007/BF00228826 PMID: 8131826
7. Semmler JG, Nordstrom MA. Influence of handedness on motor unit discharge properties and force tremor. Exp Brain Res. 1995; 104(1):115–125. https://doi.org/10.1007/BF00229861 PMID: 7621929
8. Sears TA, Stagg D. Short-term synchronization of intercostal motoneurone activity. J Physiol. 1976; 263(3):357–381. https://doi.org/10.1113/jphysiol.1976.sp011635 PMID: 1018273
9. Farina D, Negro F. Common synaptic input to motor neurons, motor unit synchronization, and force control. Exerc Sport Sci Rev. 2015; 43(1):23–33. https://doi.org/10.1249/JES.0000000000000032 PMID: 25390298
10. Dideriksen JL, Falla D, Bækgaard M, Mogensen ML, Steimle KL, Farina D. Comparison between the degree of motor unit short-term synchronization and recurrence quantification analysis of the surface EMG in two human muscles. Clinical Neurophysiology. 2009; 120 (12): 2086–2092. https://doi.org/10.1016/j.clinph.2009.09.011 PMID: 19828371
11. Kirkwood PA. On the use and interpretation of cross-correlations measurements in the mammalian central nervous system. J Neurosci Methods. 1979; 1(2):107–132. https://doi.org/10.1016/0165-0270(79)90009-8 PMID: 161793
12. Nordstrom MA, Fuglevand AJ, Enoka RM. Estimating the strength of common input to human motoneurons from the cross-correlogram. J Physiol. 1992; 453:547–574. https://doi.org/10.1113/jphysiol.1992.sp019244 PMID: 1464844
13. Datta AK, Farmer SF, Stephens JA. Central nervous pathways underlying synchronization of human motor unit firing studied during voluntary contractions. J Physiol. 1991; 432:401–425. https://doi.org/10.1113/jphysiol.1991.sp018391 PMID: 1886061
14. Adams L, Datta AK, Guz A. Synchronization of motor unit firing during different respiratory and postural tasks in human sternocleidomastoid muscle. J Physiol. 1989; 413:213–231. https://doi.org/10.1113/jphysiol.1989.sp017650 PMID: 2600848
15. Kim MS, Masakado Y, Tomita Y, Chino N, Pae YS, Lee KE. Synchronization of single motor units during voluntary contractions in the upper and lower extremities. Clin Neurophysiol. 2001; 112(7):1243–1249. https://doi.org/10.1016/s1388-2457(01)00549-1 PMID: 11516736
16. Bremner FD, Baker JR, Stephens JA. Effect of task on the degree of synchronization of intrinsic hand muscle motor units in man. J Neurophysiol. 1991; 66(6):2072–2083. https://doi.org/10.1152/jn.1991.66.6.2072 PMID: 1812237
17. Huesler EJ, Hepp-Reymond M-C, Dietz V. Task dependence of muscle synchronization in human hand muscles. Neuroreport. 1998; 9(10):2167–2170. https://doi.org/10.1097/00001756-199807130-00003 PMID: 9694193
18. Semmler JG, Nordstrom MA. Motor unit discharge and force tremor in skill- and strength-trained individuals. Exp Brain Res. 1998; 119(1):27–38. https://doi.org/10.1007/s002210050316 PMID: 9521533
19. Sturm H, Schmied A, Vedel JP, Pagni S. Firing pattern of type-identified wrist extensor motor units during wrist extension and hand clenching in humans. J Physiol. 1997; 504 (Pt 3):735–745. https://doi.org/10.1111/j.1469-7793.1997.735bd.x PMID: 9401979

20. Milner-Brown HS, Stein RB, Lee RG. Synchronization of human motor units: possible roles of exercise and supraspinal reflexes. Electroencephalogr Clin Neurophysiol. 1975; 38(3):245–254. https://doi.org/10.1016/0013-4694(75)90245-x PMID: 46802

21. Schmied A, Pagni S, Sturm H, Vedel JP. Selective enhancement of motoneurone short-term synchrony during an attention-demanding task. Exp Brain Res. 2000; 133(3):377–390. https://doi.org/10.1007/s002210000421 PMID: 10958528

22. Yao W, Fuglevand RJ, Enoka RM. Motor-unit synchronization increases EMG amplitude and decreases force steadiness of simulated contractions. J Neurophysiol. 2000; 83(1):441–452. https://doi.org/10.1152/jn.2000.83.1.441 PMID: 10634886

23. Lippold OC, Redfearn JW, Vuco J. The rhythmical activity of groups of motor units in the voluntary contraction of muscle. J Physiol. 1957; 137(3):473–487. https://doi.org/10.1113/jphysiol.1957.sp005828 PMID: 13463782

24. Dietz V, Bischofberger E, Wita C, Freund HJ. Correlation between the discharges of two simultaneously recorded motor units and physiological tremor. Electroencephalogr Clin Neurophysiol. 1976; 40(1):97–105. https://doi.org/10.1016/0013-4694(76)90183-8 PMID: 55352

25. McAuley JH, Rothwell JC, Marsden CD. Frequency peaks of tremor, muscle vibration and electromyographic activity at 10 Hz, 20 Hz and 40 Hz during human finger muscle contraction may reflect rhythmicities of central neural firing. Exp Brain Res. 1997; 114(3):525–541. https://doi.org/10.1007/p100005662

26. Halliday DM, Conway BA, Farmer SF, Rosenberg JR. Load-independent contributions from motor-unit synchronization to human physiological tremor. J Neurophysiol. 1999; 82(2):664–675. https://doi.org/10.1152/jn.1999.82.2.664 PMID: 10444664

27. Taylor AM, Steege JW, Enoka RM. Motor-unit synchronization alters spike-triggered average force in simulated contractions. J Neurophysiol. 2002; 88(1):265–276. https://doi.org/10.1152/jn.2002.88.1.265 PMID: 12091552

28. Kernell D, Eerbeek O, Verhey BA. Relation between isometric force and stimulus rate in cat's hindlimb motor units of different twitch contraction time. Exp Brain Res. 1983; 50(2–3):220–227. https://doi.org/10.1007/BF00239186 PMID: 6227493

29. Celichowski J, Grottel K. Sensitivity of the motor unit unfused tetanus to changes in the pattern of motoneuronal firing. Arch Ital Biol. 2001; 139(4), 329–336. PMID: 11603076

30. Grottel K, Celichowski J. The influence of changes in the stimulation pattern on force and fusion in motor units of the rat medial gastrocnemius muscle. Exp Brain Res. 1999; 127(3):298–306. https://doi.org/10.1007/s002210050799 PMID: 10452217

31. Fuglevand AJ, Winter DA, Patla AE. Models of recruitment and rate coding organization in motor-unit pools. J Neurophysiol. 1993; 70(6):2470–2488. https://doi.org/10.1152/jn.1993.70.6.2470 PMID: 8120594

32. Santello M, Fuglevand AJ. Role of across-muscle motor unit synchrony for the coordination of forces. Exp Brain Res. 2004; 159(4):501–508. https://doi.org/10.1007/s00221-004-1975-1 PMID: 15558252

33. Raikova R, Aladjov H, Celichowski J, Krutki P. An approach for simulation of the muscle force modeling it by summation of motor unit contraction forces. Computational and Mathematical Methods in Medicine, 2013 Vol. 2013, Article ID 625427. https://doi.org/10.1155/2013/625427 PMID: 24198849

34. Raikova R, Celichowski J, Angelova S, Krutki P. A model of the rat medial gastrocnemius muscle based on inputs to motoneurons and on an algorithm for prediction of the motor unit force. J Neurophysiol. 2018; 120(4):1973–1987. https://doi.org/10.1152/jn.00041.2018 PMID: 30020845

35. Raikova R, Pogrzebna M, Drzymała H, Celichowski J, Aladjov H. Variability of successive contractions subtracted from unfused tetanus of fast and slow motor units. J Electromyogr Kinesiol. 2008; 18(5):741–751. https://doi.org/10.1016/j.jelekin.2007.02.010 PMID: 17419073

36. De Luca CJ, Erim Z. Common drive of motor units in regulation of muscle force. Trends Neurosci. 1994; 17(7):299–305. https://doi.org/10.1016/0166-2236(94)90064-7 PMID: 7524216

37. Raikova R, Celichowski J, Krutki. A general mathematical algorithm for predicting the course of unfused tetanic contractions of motor units in rat muscle. Plos One. 2016 11(9):e0162385. https://doi.org/10.1371/journal.pone.0162385 PMID: 27622581

38. Chase CI. Computation of variance accounted for in multiple correlation. The Journal of Experimental Education. 2015, 28(3):265–266.

39. Torres-Oviedo G, Macpherson JM, Ting LH. Muscle synergy organization is robust across a variety of postural perturbations. J Neurophysiol. 2006; 96: 1530–1546. https://doi.org/10.1152/jn.00810.2005 PMID: 16775203

40. Okada K. Negative estimate of variance-accounted-for effect size: How often it is obtained, and what happens if it is treated as zero. Behav Res Methods. 2017; 49(3):979–987.

41. Loeb GE, Yee WJ, Pratt CA, Chanaud CM. Cross-correlation of EMG reveals widespread synchronization of motor units during some slow movements in intact cats. J Neurosci Method. 1987; 239–249. https://doi.org/10.1016/0165-0270(87)90119-1 PMID: 3682877

42. Kline JC, De Luca CJ. Synchronization of motor unit firings: an epiphenomenon of firing rate characteristics not common inputs. J Neurophysiol. 2016; 115(1):178–192. https://doi.org/10.1152/jn.00452.2015 PMID: 26490288

43. Semmler JG. Motor unit synchronization and neuromuscular performance. Exerc. Sport Sci. Rev. 2002; 30(1):8–14. https://doi.org/10.1097/00003677-200201000-00003 PMID: 11800501

44. Logigian EL, Wierzbicka MM, Bruyninckx F, Wiegner AW, Shahahi BT, Young RR. Motor unit synchronization in physiologic, enhanced physiologic and voluntary tremor in man. Ann Neurol. 1988 Mar; 23 (3):242–250. https://doi.org/10.1002/ana.410230306 PMID: 2967666

45. Gallego JA, Dideriksen JL, Holobar A, Ibáñez J, Pons JL, Louis ED, Rocon E, Farina D. Influence of Common Synaptic Input to Motor Neurons on the Neural Drive to Muscle in Essential Tremor. J Neurophysiol. 2015; 113(1):182–191. https://doi.org/10.1152/jn.00531.2014 PMID: 25274343

46. Seburn KL, Cope TC. Short-term afferent axotomy increases both strength and depression at Ia–motoneuron synapses in rat. J Neurosci. 1998; 18(3):1142–1147. https://doi.org/10.1523/JNEUROSCI.18-03-01142.1998 PMID: 9437034

47. Mottram CJ, Wallace CL, Chikando CN, Rymer WZ. Origins of spontaneous firing of motor units in the spastic-paretic biceps brachii muscle of stroke survivors. J Neurophysiol. 2010; 104(6): 3168–3179. https://doi.org/10.1152/jn.00463.2010 PMID: 20861443

48. Zijdewind I, Thomas CK. Firing patterns of spontaneously active motor units in spinal cord injured subjects. J Physiol. 2012; 590:1683–1697. https://doi.org/10.1113/jphysiol.2011.220103 PMID: 22310313

49. Putney J, Conn R, Sponberg S. Precise timing is ubiquitous, consistent, and coordinated across a comprehensive, spike-resolved flight motor program. PNAS 2019; 116 (52): 26951–26960.

50. Burke RE, Rudomin P, Zajac FE. Catch property in single mammalian motor units. Science. 1970; 168:122–124. https://doi.org/10.1126/science.168.3927.122 PMID: 5417051

51. Burke RE, Rudomin P, Zajac FE. The effect of activation history on tension production by individual muscle units. Brain Res. 1976; 109: 515–529. https://doi.org/10.1016/0006-8993(76)90031-7 PMID: 1276932

52. Celichowski J, Raikova R, Aladjov H, Krutki P. Dynamic changes of twitch-like responses to successive stimuli studied by decomposition of motor unit tetanic contractions in rat medial gastrocnemius. J Neurophysiol. 2014; 112 (31):3116–3124.

53. Burke RE, Rymer WZ, Walsh JV. Relative strength of synaptic input from short latency pathways to motor units of defined type in cat medial gastrocnemius. J Neurophysiol. 1976; 39: 447–458. https://doi.org/10.1152/jn.1976.39.3.447 PMID: 181542

54. Burke RE, Jankowska E, Bruggencate G. A comparison of peripheral and rubrospinal synaptic input to slow and fast twitch motor units of triceps surae. J Physiol. 1970; 207: 709–732. https://doi.org/10.1113/jphysiol.1970.sp009090 PMID: 5499743

55. Alstermark B, Sasaki S. Integration in descending motor pathways controlling the forelimb in the cat. 14. Differential projection to fast and slow motoneurones from excitatory C3-C4 propriospinal neurones. Exp Brain Res. 1986; 63: 530–542. https://doi.org/10.1007/BF00237476 PMID: 3019752

56. Novak T, Newell KM. Physiological Tremor (8–12 Hz Component) in Isometric Force Control. Neurosci Lett. 2017; 641:87–93. https://doi.org/10.1016/j.neulet.2017.01.034 PMID: 28109777

57. McAuley JH, Marsden CD. Physiological and pathological tremors and rhythmic central motor control. Brain. 2000; 123 (8): 1545–1567. https://doi.org/10.1093/brain/123.8.1545 PMID: 10908186

58. Burke RE, Levine DN, Salcman M, Tsairis P. Motor units in cat soleus muscle: physiological, histochemical and morphological characteristics. J Physiol. 1974; 238(3):503–514. https://doi.org/10.1113/jphysiol.1974.sp010540 PMID: 4277582

59. Burke RE, Levine DN, Tsairis P, Zajac FE. Physiological types and histochemical profiles in motor units of the cat gastrocnemius. J Physiol. 1973; 234(3):723–748. https://doi.org/10.1113/jphysiol.1973.sp010369 PMID: 4148752

60. Kryściak K, Majerczak J, Kryściak J, Łochyński D, Kaczmarek D, Drzymała-Celichowska H, Krutki P, Gawedzka A, Guzik M, Korostynski M, Szkutnik Z, Pyza E, Jarmuszkiewicz W, Zoladz JA, Celichowski J. Adaptation of motor unit contractile properties in rat medial gastrocnemius to treadmill endurance training: relationship to muscle mitochondrial biogenesis. PLoS ONE. 2018; 13(4): e0195704. https://doi.org/10.1371/journal.pone.0195704 PMID: 29672614

61. Łochyński D, Kaczmarek D, Mrówczyński W, Warchoł W, Majerczak J, Karasiński J, Korostyński M, Żołądź J, Celichowski J. Contractile properties of motor units and expression of myosin heavy chain

isoforms in rat fast-type muscle after volitional weight-lifting training. J Appl Physiol. 2016; 121(4):858–869. https://doi.org/10.1152/japplphysiol.00330.2016 PMID: 27539495

62. Drzymała-Celichowska H, Krutki P, Celichowski J. Summation of motor unit forces in the rat medial gastrocnemius muscle. J Electromyogr Kinesiol. 2010; 20(4):599–607. https://doi.org/10.1016/j.jelekin.2010.01.006 PMID: 20185336

63. Celichowski J, Grottel K. The dependence of the twitch course of medial gastrocnemius muscle of the rat and its motor units on stretching of the muscle. Arch Ital Biol. 1992; 130(4):315–324. PMID: 1489250